June 2021

Mapping Plastic Pollution in the Amite Watershed, Louisiana

Gourav Divan

MAPPING PLASTIC POLLUTION IN THE AMITE WATERSHED, LOUISIANA

A Thesis

Submitted to the Graduate Faculty of the
Louisiana State University and
Agricultural and Mechanical College
in partial fulfillment of the
requirements for the degree of
Masters of Science

in

The Department of Environmental Sciences

by
Gourav Deepakraj Divan
B.S., Louisiana State University; 2019
August 2021

Acknowledgements

Foremost, I am endlessly grateful to my advisor, Dr. De Jesus Crespo, for helping me throughout this process. Thank you for being so understanding, encouraging, and giving me the freedom to ask questions and grow as a scientist and writer. Thank you to my committee members, Dr. Mark Benfield and Dr. Thomas Douthat, for providing their expertise, equipment, and suggestions throughout this experience. Thank you as well to Ana Trujillo, and the Scuba Dogs Society for giving me an incredible crash course into microplastics, sampling and education.

The completion of this thesis would not have been possible without the support and encouragement from my family and friends. Thank you for your endless patience and willingness to push me forward even when I was ready to give up. Special thanks to my sister Amruta, Samay, Rohan, Karishma, and Arjun, for being my cheerleaders. Thank you to my cohort members in both undergrad and graduate school: Leah, Xavier, Kalvin, Victoria, Lindsey, and Callie, and my undergraduate worker for assisting me with sampling. Lastly, thank you to PN, for sticking by my side and giving me support and company when I needed it the most.

Table of Contents

List of Tables

List of Figures

Abstract

Microplastics have quickly emerged as a concerning pollutant in both freshwater and marine environments. Their recent discovery means that their impacts are still being studied, however, it is important to continuously monitor their concentrations. An important conduit of plastic pollution to marine environments are rivers and streams. Previous models have estimated the transport of plastics from land to sea in many parts of the world. Most of these models, however, have been conducted at coarse spatial resolutions that make it difficult to establish tractable management programs to minimize this impact. Here, a previously existing model was applied to model for microplastic emissions from rivers to sea (Lebreton et al., 2017) in the Amite Watershed using population density, watershed distribution, and dams as inputs. To validate this model, six different streams were selected and sampled at along the Amite River with a gradient of predicted microplastic exports. For this in-situ sampling, a simple and economically viable sampling method was chosen for three months of sampling (October, November, and December). The expected result was that the observed values from the in-situ sampling would correlate with the predicted model's output. The model's predicted waste outputs for the Amite watershed ranged from 3.33E-6 to 4.89E+3 kg/day. In general, predicted values were at a discrepancy from the observed values. Two sites sampled at (Mill Creek and Clay Cut Bayou), showed higher (observed being 8.78E-3 kg/day while the model predicted 8.28E-7 kg/day) and lower (observed being at 1.22E-2 kg/day while the model predicted the output to be 2.60E-2 kg/day) than expected values respectively, potentially due to the stream conditions and the sampling method chosen which did not account for microplastics caught in sediments. These discrepancies suggest that the sampling method chosen may not be adequate for microplastic analysis in the Amite River watershed. The modeling approach applied is easy

to replicate and offers a first glimpse of potential plastic pollution hotspots at the sub watershed level. However, the results of the in-situ study suggest a need for further model validation efforts using alternative methods of plastic sampling that include sediment sampling for better characterizing slow moving waters in Louisiana. This study also highlights the potential need for incorporating other important spatial predictors of plastic pollution, aside from population and runoff. Recommendations for future studies include improving modelling and sampling accuracy for microplastics.

1. Introduction.

1.1 Plastic Waste.

Plastics, along with metal and rubber, are the most common types of marine debris found in our oceans and waterways (NOAA 2020). It was estimated that a total of 275 million metric tons (MMT) of plastic waste was generated in coastal countries in 2010, with 4.8-12.7 MMT entering the ocean itself (Jambeck et al. 2015). The top 5 countries that are estimated to produce the most amount of mismanaged plastic waste are China (1.3-3.5 MMT/year), Indonesia (.5-1.3 MMT/year), Philippines (.3-.8 MMT/year), Vietnam (.3-.7 MMT/year), and Sri Lanka (.2-.6 MMT/year), with the United States ranking as the 20th highest mismanaged waste producing nation (producing 0.04-.11 MMT/year) (Jambeck et al. 2015). Marine plastic waste itself, though, is not monolithic, and can be classified based on its physical and chemical properties.

Marine plastic waste comes in all shapes and sizes and is categorized based off their size. Plastic waste particles larger than 5 mm are classified as macroplastics, while plastic particles that are 5 mm or smaller in length are classified as "microplastics" (Parker 2013). Microplastics can be arranged into several categories, such as foams, beads/nurdles, fibers, fragments and films. Microbeads are spherical polyethylene plastics that are added as exfoliants in cleansers, and cosmetics (Flowers 2016). Fibers are products from larger items like clothing, diapers, and cigarette butts (Flowers 2016). Fragments break off from larger pieces of plastic like cutlery, lids, or single use products as a result of physical and chemical break down processes (Flowers 2016). Nurdles are plastic pellets which are used to manufacture larger plastic goods (Flowers 2016).

Macroplastics can become microplastics through three ways, classified as physical, chemical, and biological degradation. Physical and chemical degradation, or abiotic degradation,

usually proceed biological degradation due to the poor bioavailability of marine plastic particles. Abiotic methods of degradation can include photodegradation (caused by sunlight), thermal degradation (caused by heat or cold), and mechanical degradation (due to wave interactions) (Zhang et al. 2021). Biotic, or biological, degradation refers to the deterioration of plastics by organisms. Microorganisms, such as bacteria, fungi, and insects, are primarily responsible for the biological degradation of particles (Crawford and Quinn 2017).

Plastic waste in marine ecosystems is primarily found in areas next to large cities and offshore canyons, as waste is trapped in zones with high sedimentation rates, and these rates are common where the seafloor is relatively flat (Galgani et al. 2000). In addition, coastal areas with industrial activities such as harbors are regarded as hotspots for improper waste disposal (Galgani et al. 2000). Gyres are also particular hotspots for both macroplastic and microplastic accumulation, as plastic waste lacks the ability to exit a gyre after entering it. The abundance of plastic debris in gyres comes from fishing gear followed by land-based sources, with plastic moving from land to sea, and then entering currents which end up in gyres (Li et al. 2016).

1.2. Fate of Plastics.

The most common types of plastic waste found in marine ecosystems are polyesters (PES), followed by polyethylenes (PE), polyvinyl chlorides (PVC), low density polyethylenes (LDPE), polypropylene (PP), polystyrene (PS), polycarbonates (PC), and polycarbonate/acrylonitrile blends (PC/ABS) (Li et al. 2016). The different types of plastic waste have different specific gravities, or the ratio of density of a substance in comparison to the density of water (SG = 1.0). A plastic type's specific gravity indicates how quickly it will sink in marine ecosystems, and in turn, dictates the fate of a microplastic (whether it will continue to be suspended in surface water, or sink to the sediment layer. It is important to note that sediment

layers for both freshwater and marine ecosystems have been established to be sinks for microplastics (Kowalski et al. 2016)

PESs are used as fibers for textiles, or as the material used for plastic bottles, jars, film, packaging and tubing, and have a high specific gravity which lets them sink quickly (the ratio of density of a substance in comparison to the density of water [SG = 1.00]) (SG = 1.37-1.40). PVCs are used primarily for plumbing, piping and guttering purposes. They have a plethora of health effects, such as eye damage and skin damage if ingested or inhaled for a long time (Akovali 2012) and have a specific gravity of 1.38. PCs are used for compact discs and for eye wear and lenses. Bisphenol-A can be leached from PCs, which can cause heavy metal poisoning and changes to liver function (Srivastava & Godara 2013), their specific gravity ranges in between 1.20 to 1.22. PEs are used in a wide range of cheap products, such as plastic bags and bottles, and have a specific gravity in between 0.91-0.96 (Li et al. 2016). LDPEs are used in detergent bottles, milk jugs, tubes and some pipes and insulation. They have the ability to release estrogenic chemicals that causes changes in the structure of human cells and have a specific gravity of 0.94. PPs are used as bottle caps, drinking straws, and small food containers (Karian 2003), they are relatively light, with a specific gravity range of 0.83-0.85 (Li et al. 2016). PSs are used as packing foam, food containers, and plastic tableware. They can cause eye, nose, and throat irritation if ingested and have the ability to be stored as body fat. Their specific gravity is 1.05. PC/ABSs are a blend of PC and ABS that is used for vehicle interior and exterior parts and for cell phone bodies (Wang et al. 2007). Their specific gravity is 1.10 (Li et al. 2016).

1.3. Impacts of Plastics.

Microplastics have the ability to adsorb and carry inorganic and organic chemical pollutants along with heavy metal pollutants through freshwater ecosystems (Liu et al. 2019, Naqash et al. 2020, Rios et al. 2007). To understand how microplastics can impact organisms and humans, we first must understand how pollutants are transported through the water column and how available microplastics are to adsorbing, or carrying without absorbing, them. Pollutants are introduced to marine ecosystems through point source and non-point source pollution. From there, the sorption capability of microplastics with persistent organic pollutants (POPs) are dependent on the concentration of contaminants in the water column, as opposed to the salinity of the waterway (Bakir et al. 2014). The desorption rates for POPs on microplastics is also dependent on retention time in marine ecosystems and are also not affected by salinity (Bakir et al. 2014).

Sorption mechanics of microplastics for inorganic and organic pollutants are dependent on the age of the microplastic piece in the water column, as older microplastics have been recorded to adsorb hydrophilic and hydrophobic chemicals, as opposed to just hydrophobic pollutants (Liu et al 2019). In addition, the adsorption ability of microplastics depends on the type of plastic as well, with aged polystyrene being the most receptive to hydrophilic compounds, followed by aged PVC, PVS, and then PS (Liu et al. 2019). Organic pollutants, like inorganic pollutants, are able to adsorb to microplastic particles. One study suggests that polychlorinated biphenyls (PCBs, once commonly used as a coolant fluid) were the most common POPs to adsorb to microplastics (Rios et al. 2007). In addition, the concentration of POPs on plastic debris is dependent on the age of the plastic, as the older a plastic particle may be, the more POPs will be on its surface (Mato et al. 2001).

Along with inorganic and organic pollutants, heavy metals have been recorded to be adsorbed by microplastics. Heavy metals, considered soluble toxic pollutants, have the ability to bioaccumulate not only in aquatic organisms, but in humans as well. These heavy metals can include cadmium, cobalt, copper, chromium, nickel, lead and zinc, with polyethylene and polyvinyl chloride microplastics reporting significant adsorption those heavy metals (Naquash et al. 2020). Like organic and inorganic pollutants, heavy metal's sorption onto microplastics is dependent on their age, as older microplastics can sorb heavy metals better than younger and less degraded microplastics can (Naquash et al. 2020). Lastly, PP and PE based microplastics are able to accumulate contaminants, perhaps due to its permeable lipophilic nature.

Macroplastics and microplastics have the ability to affect organisms living in water columns in direct and indirect ways. Direct impacts for both can include ingestion, while indirect impacts for both include bioaccumulation due to toxin sorption in all trophic levels and habitat creation. Marine organisms have confused plastic pollutants for food. Marine turtles have mistaken plastic objects for food items, as transparent polyethylene bags evoke the same feeding response in sea turtles as jellyfish do (Wehle & Coleman 1983). Marine fauna could also be physically affected by plastic debris by being tied up or choked by them (Worm et al. 2017). For example, gulls and sea turtles have been found with plastic six-pack straps caught around their necks, causing difficulty to digestion and breathing (Wehle & Coleman 1983). Microplastic debris can also accumulate in the planktonic larvae of crustacean species, as several are susceptible to microfiber exposure, with gut content analyses revealing fibers in *Nephrops norvegicus* (Wright et al. 2013). In addition, zooplankton ingesting microplastics contribute to the carbon transfer to deeper waters. The sinking rate of their fecal matter is slowed down 2.25-fold due the presence of microplastics and their low density (Galloway et al 2017). Fish that have

ingested microplastics laden with heavy metals have had hindered predatory performances, as heavy metal poisoning caused severe oxidative stress and deteriorated brain functions (Naquash et al. 2020). Microplastic accumulation can also affect population structures, as pelagic insects (*Halobates serceus*) are now able to proliferate in benthic microplastic sinks, as they are no longer restricted by the lack of hard substrate (Wright et al. 2013). In freshwater ecosystems, caddisfly larvae have been observed to use microplastic particles as a part of their casing (Tibbetts et al. 2018). Because of all the documented and potential impacts that plastics may pose in marine ecosystems, waste management to reduce this pollution problem is becoming increasingly important.

1.4. Management of Plastics.

The management of plastic waste in the United States for both marine and freshwater ecosystems began in the 1970s and 1980s, with the introduction of the Marine Protection, Research and Sanctuaries Act (MPRSA) of 1972 and the Marine Dumping Ban Act of 1988. The MPRSA aimed to regulate the intentional disposal of materials in the ocean and authorize research related to material disposal in the ocean, while the Ocean Dumping Ban Act prohibited the dumping of municipal sewage sludge and industrial waste into the ocean. These two acts of legislature were spurred by the 1972 Convention on the Prevention of Marine Pollution by Dumping of Wastes and Other Matters. There, 85 countries agreed to the prohibition of dumping in the ocean of several heavy metals, DDT, PCBs, solid waste, oil, radioactive waste, and chemical and biological warfare agents.

The Clean Water Act (CWA) was enacted in 1972 to govern and regulate water pollution and quality in the United States (33 U.S.C. §1251-1387, 1972). Its objective is to restore and maintain the integrity of the nation's waters, gives some responsibility to the states to address

pollution with allowing for federal assistance in pollution cleanups if the states ask for it. The CWA was expanded using the Clean Water Rule in 2015. This rule clarifies water resource management in the United States, defining what the scope of federal protection is over streams and wetlands. These bodies of water are now referred to as the Waters of the United States (WOTUS). In addition, the CWA has been successful at reducing point source pollution, pollution that originates at a single, identifiable source. Its success relies on state agencies enforcing federal level rules, these state agencies enforcing rules such as issuing emission permits to polluters and monitoring pollution emissions.

In 2015, the Microbead-Free Waters Act, enacted by congress, prohibited the manufacturing, packaging, and distribution of plastic microbes in rinse off cosmetics (such as skincare products and body washes) (80 FR 37053, 2015). In 2019, the Clean Water Rule was formally repealed by the Trump administration. A replacement rule was issued in 2020, which rolled back on protections to certain wetlands and streams and eliminating all requirements for landowners to get EPA approval for land modifications (85 FR 22250, 2020). Even though these two acts have been enacted recently, there is still a fair amount of plastic waste in the United States' waterways. As of April 2021, the Biden administration is racing to reverse the replacement rule before it is being put into effect.

A primary source for smaller microplastics in waterways is treated wastewater. Larger residual microplastics are usually removed from wastewater before discharge into streams through filtering methods with high capture efficiency, however, smaller microplastics have the ability to slip through filtration systems used in wastewater treatment methods (Freeman et al. 2020).

1.5. Monitoring of Plastics.

There are several methods for plastic debris monitoring and analysis, which vary by the type of ecosystem being evaluated and the objectives. In saltwater/ocean ecosystems, neuston nets have been towed or allowed to stay suspended parallel to the flow of the waterway for a set period of time to collect microplastics in the surface water region. This method, however, has resulted in the underestimation of the extent of microplastic pollution, as it does not account for smaller microplastics that can pass through the sampling net (Barrows et al. 2017). To curb this, grab sampling methods have been developed, where samples are collected in glass jars and then are immediately capped underwater to reduced air exposure time. It was confirmed that net tow methods were useful for collecting larger microplastics pieces, while grab sampling allowed for the collection of microplastics at a larger density with a greater diversity of microplastics (Barrows et al. 2017).

Once sampled for, microplastic can be characterized by their physical and chemical traits. The physical analytical methods used to identify microplastics would be through microscopy. The chemical analytical methods can include spectroscopy and thermal analysis, with procedures branching off those two method types (Shim et al. 2017). Microscopy is a widely used method for identification and is used to identify plastic-like particles. Microscopy, though accessible, runs into the risk of not having the ability to characterize plastics with high accuracy. Polarization, a subset of microscopy, is successful in the identification of polyethylene particles. Fourier Transform Infrared (FTIR) spectroscopy, on the other hand, works by shining infrared light through samples and measuring how much light the sample absorbs at each wavelength. It is not only very efficient at identifying microplastics, but it has the ability to identify the type of carbon-based polymers in the plastic. Transmission, reflectance, and attenuated total reflection

(ATR) modes for FTIR machines are all able to identify microplastics in samples. Raman spectroscopy also uses a similar method, by shooting a laser beam at an object and recording the different frequencies of back scatter depending on the molecular structure and atoms present, unique to different types of polymers (Shim et al. 2017). Thermal analysis of microplastics can be used to identify the physical and chemical properties of microplastics depending on their stability in thermal changes. This method, though useful, requires reference materials and an understanding of the polymer type before using thermal methods (Shim et al. 2017). In addition, this method is destructive and prevents for repeated analysis of microplastic samples. Gas chromatography, a method of thermal microplastic analysis, separates compounds in a mixture by injecting gas samples into a carrier, mobile gas phase, and passing the gas through a stationary phase. Gas chromatography also results in the destruction of its samples but results in an understand of the polymer type after analysis (Shim et al. 2017).

Microplastics can also be analyzed for through dying methods. Nile Red (NR), a fluorescent dye, has been used to stain hydrophobic microplastic particles, binding to its neutral lipids (Shim et al. 2017). The downside of using fluorescent dyes for microplastics is that organic materials can be dyed with NR. Thus, you have to remove any organic materials from microplastic samples before dying the samples with NR. Ideally, the combination of dying microplastics with NR and using FTIR spectroscopy would result in comprehensive microplastic analyses (Shim et al. 2017), that helps provide accuracy to microscopy identification.

1.6. Study Rationale and Objectives.

It has been suggested that the majority of marine plastic pollution comes from land-based sources (Worm et al. 2017). Rivers, wastewater outflows, and tides can carry plastics from cities into the ocean (Worm et al. 2017). Therefore, the management of non-point sources of plastic

inland should be part of management efforts to reduce plastic pollution sources to the world's oceans. Identifying potential hotspots of plastic sources, would help facilitate management efforts towards this purpose.

To address this, previous studies (Jambeck et al. 2015, Lebreton et al. 2017) have developed models to predict the amount of plastic waste entering from land to the ocean across the world's rivers. Both of these studies are based on the premise that there is a positive correlation between the number of people and the number of plastics found in surrounding waterways. Jambeck et al. (2015) modeled plastic transport in coastal areas using estimates of mismanaged waste and estimates of coastal populations density. Lebreton et al. (2017) applied some of the same estimates, but also included other important factors, such as estimates of in-land population upstream, and hydrological factors, such as runoff and the location of potential plastic sinks (i.e., dams). While Lebreton et al (2017) improved the approach for estimating plastic inputs from rivers to sea at a global level, their estimates were based on data with very coarse spatial resolution, making it difficult to track sources and develop management plans at the local level.

In this study, I aimed to replicate Lebreton's (2017) model at a finer spatial resolution in tributaries (Hydrologic Unit Code 12) of the Amite River Watershed, Louisiana. I also attempted to validate this model's prediction using in-situ sampling within the watershed. If the model's predictions were accurate, then I hypothesized that HUC-12 watersheds with higher population density and higher runoff values will have higher concentrations of plastics in their surface waters, and this will be reflected in the in-situ sampling.

2. Study Site

2.1. Study Site Introduction

Louisiana's relationship with plastic pollution in surface waters is unique in the United States. It experiences one of the highest rates of pollution for both physical and chemical waste largely due to inputs from the Mississippi River, which drains a great proportion of the nation (Martin 2018). In addition, the Mississippi River has been the host of several plastic pollution events, the most being the spillage of nearly 750 million nurdles in August 2020. This incident was caused by a shipping container falling into the Mississippi River near New Orleans (Dermansky 2020). Several macro- and microplastic related studies have been conducted on water and organisms in the Mississippi River including a study to see how the Mississippi River and its tributaries contribute plastic pollution into the Gulf of Mexico (Scircle et al. 2020). This study was conducted to identify and quantify microplastic pollution in water and fish species found in the Mississippi, resulting in the estimation of 327 billion particles of microplastics flowing out of the Mississippi River per year, approximately weighing 811,870 kg (Toner 2020). Aside from the Mississippi River, there are other highly polluted waterways within Louisiana. Lake Maurepas, for example, is the outflow point of several rivers (Tchefuncte, Pearl, and Amite) in southeast Louisiana. It is considered the second most polluted waterway for toxic releases in the nation, receiving an estimated 2.5 million pounds of toxics every year (Inglis et al., 2014). In addition, Louisiana is the 5th ranking state in toxic waste discharge, releasing 12,811,400 lbs. of toxic waste in 2007 (Inglis et al. 2014).

2.2. Study Site Description.

Figure 1. The span of the Amite River watershed in the United States.

The Amite River is a tributary river of Lake Maurepas which flows from Mississippi to Louisiana. It is 117 miles long and originates as two forks (East Fork and West Fork) in southwest Mississippi, with the two forks meeting at the Louisiana-Mississippi state line. The river then flows south through Louisiana, passing through Livingston Parish and Denham Springs, before emptying into Lake Maurepas (USGS 2018). The Amite River watershed's land usage is largely rural and agricultural, with some suburban development surrounding the river after Hurricane Katrina and its subsequent migration in 2005 (Cowles et al. 2019). Currently,

only 11% of the Amite River watershed has been urbanized, with a majority of the urban population of the watershed being in the Baton Rouge metropolitan area. In addition, the Amite River is prone to flooding due to its flat topography and clay dominant soil (Cowles et al. 2019), seen in Louisiana floods of 2016, where up to 20 inches of rainwater flooded the Amite River and its tributaries. This flooding event caused in between $10-16 billion worth of property damage (Cowles et al. 2019). In addition to property damage, flooding could also lead to other impacts related to pollution transport in rivers. For example, flooding events can exacerbate transport of microplastics into streams (Kataoka et al. 2019) but have an inverse effect on microplastic loads in terrestrial waterways, flushing microplastic loads out from rivers and moving them towards marine systems (Hurley et al. 2018).

For this study, Amite River was focused on due to its proximity to a large city (Baton Rouge, La), its headwaters being in vegetated areas, and its discharge into the highly polluted Lake Maurepas. For the latter reason in particular, this study could be important, as it may provide baseline information for monitoring plastic waste transport from the source of the river to its mouth into Lake Maurepas and evaluate the most relevant contributing waterways.

3. Methods and Materials.

3.1. Model Approach.

My model for the Amite River expands on Lebreton 2017's model for worldwide coastal plastic pollution, or Mismanaged Plastic Waste (MPW), with updated data and applied that to the 81 Hydrologic Unit Code-12 (HUC-12) watersheds of the Amite River (Willson 2017). The initial formula used to calculate mismanaged plastic waste was done in Jambeck et al. 2015, where they classified mismanaged plastic waste as "material that is either littered or inadequately disposed… including disposal in dumps or uncontrolled landfills." (Jambeck et al. 2015). Mismanaged Plastic Waste was initially calculated for populations living within 50 kilometers of the coastline all over the world, with each country being assigned a mismanaged plastic waste constant. This constant is measured in kilograms per person per day, and for the United States, it is .007 (Jambeck et al. 2015).

To estimate the daily plastic output from each individual watershed, I used the following equation, originally formulated by Lebreton et al. 2017:

$$\mathbf{M_{out}} = (kM_{mpw}R)^a$$

Where M_{out} is the plastic output in kilograms per day, M_{mpw} is the mass of Mismanaged Plastic Waste (MPW) produced inside of the catchment downstream of any artificial barriers (for example, dams), and R is the monthly average runoff of the catchment. *k* and *a* are two regression parameters calculated initially by Lebreton et al. 2017., k=1.85*10^{-3} and a=1.52. These parameters were initially calculated from peer-reviewed studies which provided reliable estimates for the surface plastic concentrations found in each study (Lebreton et al. 2017). The

Mmpw is calculated by multiplying population density by Jambeck et al.'s 0.007 mismanaged plastic waste constant. For my study, the M_{out} was assumed to be the plastic output of each watershed, with each M_{out} being impacted by any other watershed flowing into it for the course of the Amite River watershed.

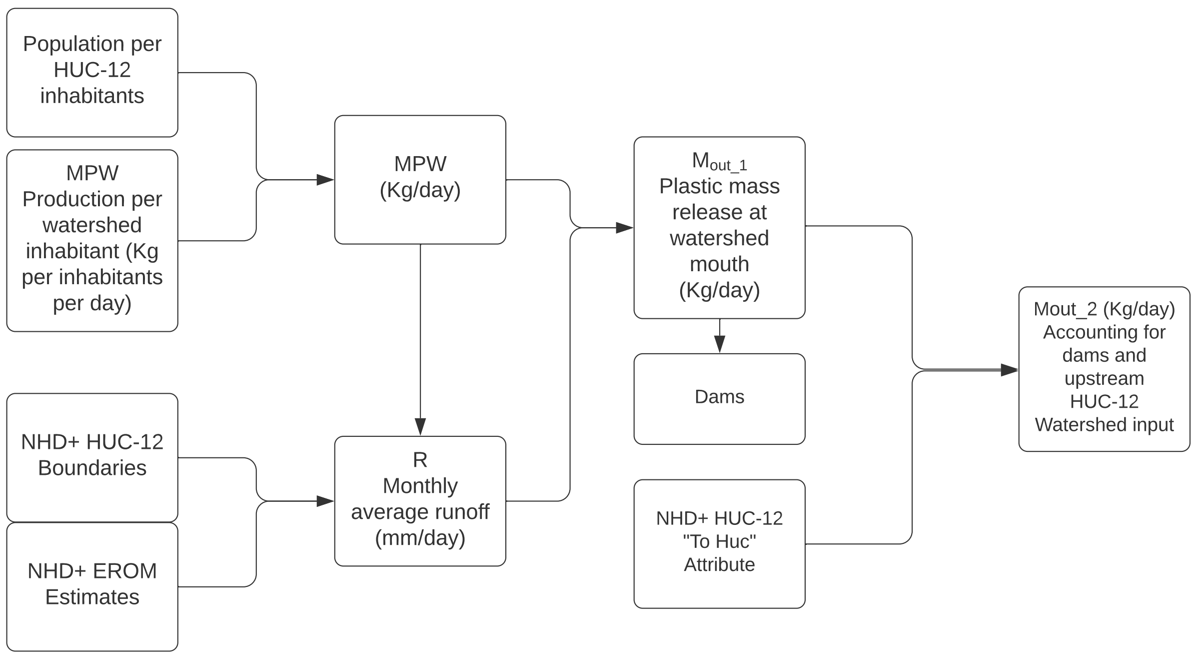

Figure 2. Framework displaying the steps taken to get the output from the model. The Hydrologic Unit Code-12 (HUC-12) boundaries and Enhanced Unit Runoff Method (EROM) estimates came from the National Hydrography Dataset (NHD+) database.

This model differs from Lebreton's, as it used updated watershed, runoff, population data; Lebreton 2017 used HUC-10, or fifth-level (watershed), data. In comparison, the updated model was able to use HUC-12, or sixth-level (subwatershed) data. Furthermore, the updated model uses a finer spatial resolution for runoff of 30 square meters, as opposed to Lebreton's more coarse spatial resolution of 0.25 degrees by 0.25 degrees, or roughly 27 kilometers squared (Gaffin et al. 2004, Yetman et al. 2004. McKay et al. 2012). The updated model's runoff data was obtained from the National Hydrography Dataset's Enhanced Unit Runoff Method (EROM). The EROM approach provides mean annuals stream flows for all flowlines in NHDPlus files and

has the capability to perform mean monthly flow and velocity estimates. NDHplus files contain three primary spatial hydrological layers: flowlines, catchment, and water bodies (McKay et al. 2012). These three features were used when calculating the plastic outputs of the watersheds studied at (McKay et al. 2012). Lastly, the updated model used population models based on census block groups (i.e. avg. 41 km^2 for the Amite watershed), in comparison to Lebreton's 15 by 15 degree population resolution, or 1665 km^2 (Sleeter & Gould 2007). For the updated model's population estimates, ArcGIS's Geospatial Research and Spatial Services Program, or GRASP, was used to calculate the population. This population estimator uses a feature of interest, census data, and the extent of user-defined data (i.e. watersheds) to calculate the proportion of each population that falls in the extent of the area defined by the user (GRASP 2018).

It is also important to note that Lebreton's population metrics, like Jambeck's, only extended 50 km into the coastline, which only allowed them to quantify their land-based plastic output from coastal populations (Lebreton et al. 2017, Jambeck et al. 2015). The updated model's study of the Amite River's watershed extends 78 miles inland to the head of the Amite River watershed.

3.2. In-Situ Sampling

3.2.1. Field sampling

Microplastic samples were collected at six sample sites throughout the Amite River watershed in both Louisiana and Mississippi. Exclusively microplastics were sampled for, as opposed to microplastics and macroplastics, to stay consistent with Lebreton's et al.'s study; several constants were developed in Lebreton et al.'s study to extrapolate macroplastic output estimates from watersheds to determine how much plastic waste was being emitted from a

watershed in kg/day. When selecting sample sites, the Amite River's sub-watersheds into low, medium, and high plastic output based on the predictive model (details below). From there, six sub watersheds were selected based on accessibility, and a predicted plastic waste output gradient, with two subwatersheds being in each category (low, medium, and high). The low output watersheds were Pumpkin Patch Creek and Mill Creek, in the east fork of the Amite River and in Central, Louisiana, respectively. The medium output sites were Cotton Creek and Days Creek, both located in the West Fork. The high output sites were Bayou Barbary and Clay Cut Bayou, located at the bottom of the watershed close to Lake Maurepas.

These samples represented low, medium, and high microplastic output watersheds according to the model, with two watersheds representing each output category. All of the sample sites were chosen due to their location at the bottom of their respective watershed and whether there were bridges going over the body of water to facilitate sampling. This sampling collection method was applied by Kataoka et al. (2019) and was considered ideal for this study,

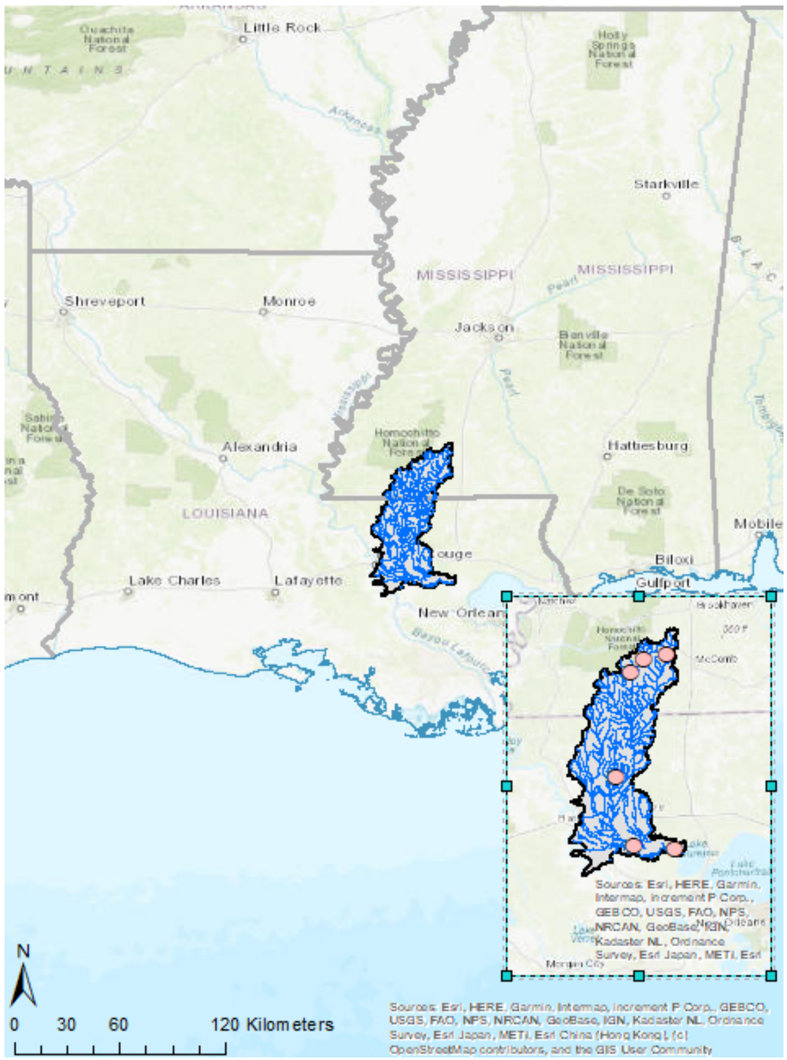

Figure 3. Inset map displaying the span of the Amite River Watershed.

because access to a boat for sampling purposes was limited. In addition, this method could be conducted safely regardless of the waterway's flooding conditions, as it did not require direct entry into the waterway. Sampling occurred in a three-day period once a month for three

consecutive months (October-December), with sample sites being paired together based on their proximity to one another.

To collect microplastic, a small plankton net (Aquatic Research Instruments, 30 cm diameter x 90 cm long plankton net equipped with a 333 micron mesh and a detachable cod end lined with 333 micron mesh was deployed from the bridge to the center of the waterway. The mesh size of 333 μm has been used by other studies (Kataoka et al. 2019, Toner 2020). Any other nets with smaller mesh sizes have been noted to become clogged with suspended materials (Kataoka et al. 2019). The net was hung off the bridge at the center of the stream for 10 minutes, with a flow meter (General Oceanics Inc. Model 2030R Flowmeter) attached to the center of the mouth of the plankton net. The net was not fixed to the water's surface, but a third of the net was allowed to be suspended above the water surface to allow for particles to flow into the net. The volume of water flowing through the net was calculated using the equation in the manual provided by General Oceanic (General Oceanic Inc. 2018):

$$\textbf{Volume in m}^{\mathbf{3}} = \Pi * (net\ mouth\ radius)^2 * (difference\ in\ counts\ *\ rotator\ constant)\ /\ 999{,}999$$

Where the *net mouth radius* is 15 cm, the *difference in counts* being the larger number reading from the flow meter - the lower number reading from the flow meter, and the *rotator constant* being 26,873 for standard speed rotators (General Oceanic Inc. 2018).

The contents of the net were then rinsed with deionized water (to remove any microplastics) and collected in the cod end. Any organic matter or suspended particles were picked out of the cod end and sprayed with pre-filtered deionized water. The runoff water in the cod net and from the organic matter spraying process was allowed to pass through a 100 μm mesh filter on site before being collected in a glass jar. The plankton net, canister, and mesh filter were rinsed down with deionized water in between sampling and after every sample site.

Figure 4. The sample net suspended in a stream due to the flow of the waterway.

Three blank samples were conducted as well, following the same procedure, but using deionized water instead of stream water to flow through the net and cod end at the bottom of the net. The blanks averaged around 6.4 m^3 of deionized water flowing through the sampling net and cod end for the 10 minutes of each sample. The results of the blanks were averaged together and subtracted from findings of the *in-situ* samples.

3.2.2. Microplastic Evaluation in the Laboratory.

The glass containers containing samples were sealed and refrigerated until the treatment and analysis procedure began. To digest organic matter from samples, 20 ml of 35% H_2O_2 was added to each sample. The sample was then set on a stir plate for 15 minutes to allow for the sample water and the H_2O_2 to be properly mixed. H_2O_2 has been used before in microplastic water samples as it reacts strongly with organic matter, breaking it down into CO_2 and water without affecting the integrity of the microplastic in the sample itself (Munno et al. 2018).

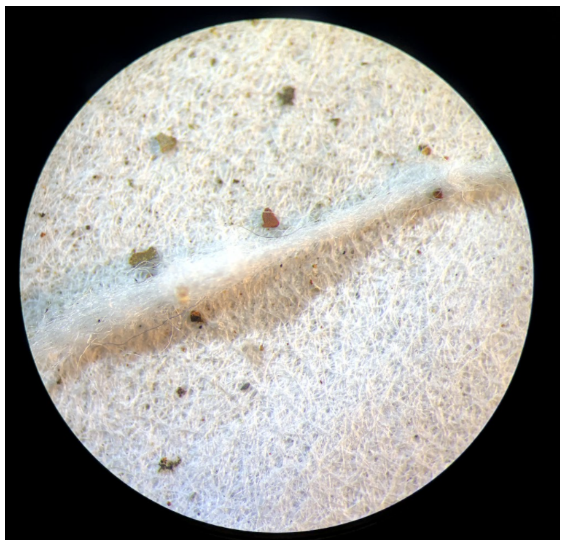

Figure 5. A microplastic caught on one of the filters after the treatment procedure.

Once the samples had been stirred, they were allowed to sit covered for at least 2 hours, or until the bubbles from the H_2O_2 reaction had subsided, indicating that the H_2O_2 reaction had completed. Post treatment, the sample was poured into a vacuum water filtration apparatus and filtered through a filter paper (Fisherbrand Filter paper, Qualitative-grade P8, Flow Rate: Fast, 5.5 cm diameter). The paper's particle retention allowed for particles in between 20-25 µm to get caught in the filter. The resulting filter was dried in an oven at 60°C for 24 hours before counting the microplastic particles that were caught in the filter (as seen in figure 3). The microplastic particles were then counted in the filter using a dissection microscope (Leica MZ6

Stereomicroscope with 6:3:1 zoom), organizing them into five categories: microfibers, microfilaments, microfragments, foam, and nurdles. These categories were determined based off color and shape indicators. Due to budget and time constraints, microscopy was the only method used for plastic identification in this study. While I was not able to supplement this analysis with FTIR or NR dyes as would be ideal, samples collected were preserved for potential future assessment using these methods. Due to this limitation, identification of plastic particles was limited to those items that could be clearly identified as plastics by shape and color, and any other particles resembling microplastics were counted as well but were not added to the total estimates of plastic particles per sample site for this study.

3.3. Statistical Analysis.

Observed values were compared to model prediction values (Mout_1, and Mout_2) using simple linear regressions. Linear regressions were also used to test the relationship between the observed plastics values and the models raw input variables, specifically the HUC-12 population, and average runoff. I tested the role of site type (High, Medium, Low), and sampling month (October, November, December) on the observed plastic values using a 2-Way ANOVA. All variables were scaled prior to analysis using the sample means and standard deviations (R Core Team 2017). Model residuals were analyzed for normality using Shapiro Wilks Normality tests. All analyses were conducted in R (R Core Team, 2020).

Chapter 4. Results.

4.1. Modelling Approach

According to the generated model, there is an estimated total of 346,643 kilograms of plastic that flows through the Amite River watershed per year, with an average total of 950 kilograms of plastic per day. The model's outputs for the individual watershed's outputs, Mout_1, and outputs influenced by upstream watersheds, or Mout_2, are displayed as Figures 6 and 7, respectively. In addition, the full output of the model is seen in the appendix.

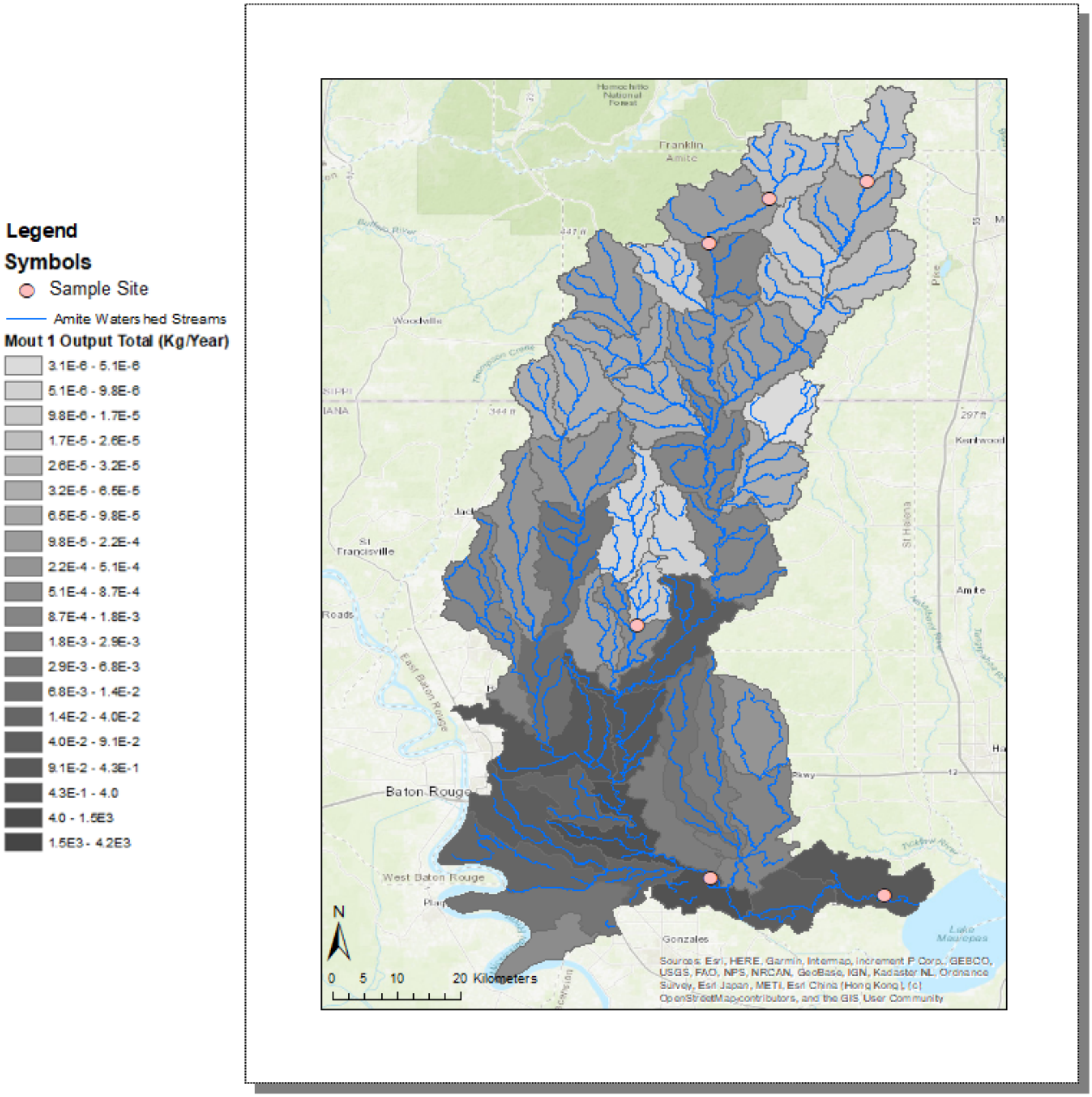

Figure 6. Plastic waste output (kg/year) of every HUC-12 subwatershed in the Amite River watershed. The plastic waste output of this figure is for the individual sub-watershed (i.e.Mout_1), not accounting for sub-watershed cumulative contributions.

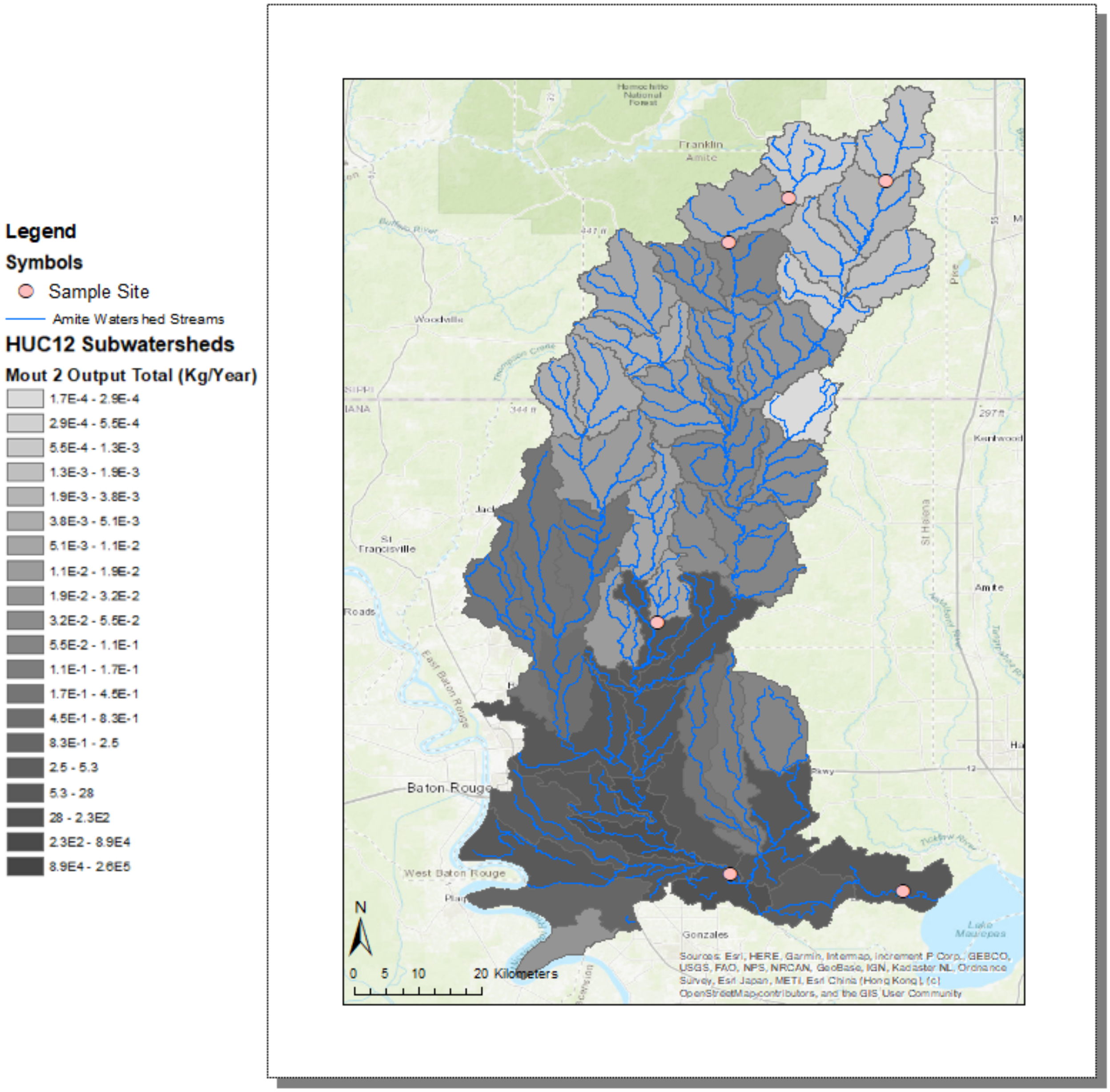

Figure 7. Plastic waste output (kg/year) of every HUC-12 subwatershed in the Amite River watershed. The plastic waste output of this figure is the Mout_2, which accounts for the cumulative sub-watershed plastic waste flows from upstream to downstream.

4.2. In-Situ Sampling

Microfibers were primarily found throughout all the sample sites, followed by a few micro fragments and microfilaments. No nurdles or foam particles were identified in any of the samples, potentially due to the microbead ban from the Clean Water Rule of 2015. Microplastic density by site and by sample did not correlate to their respective watershed's population. There was also a large amount of variability in microplastics counted from sample to sample in each triplicate, and from one month's sampling to the next. For a majority of the samples, there was a very low flow. However, at Pumpkin Patch, Days, and Cotton Creeks during the December sampling period, a large flow was seen as a result of a precipitation event the day prior to sampling. A chart playing the Amite River's discharge and the average weekly runoffs for the sample sites are seen in the Appendix (Figure 16, Table 7, respectively) (USGS 2021).

The sample sites averaged about 15 microplastic particles per sample, or about 0.04 g of microplastics per sample. In the absence of measured macroplastics due to the sampling approach, estimates of macroplastic values were predicted based on the Lebreton et al. 2017 constants to be 0.10 g per sample. Three blank samples were conducted, where the sampling procedure was run from start to finish but used deionized water instead of stream water to flow through the net and cod end. The blank samples results were averaged together and subtracted from the observed mass of plastics. After this correction was made, a few of the averages of tthe resulting masses ended up being smaller than 0, those less than 0 numbers being bolded in the Tables 1, 2, and 3.

The microplastic concentrations had their triplicate values averaged and have been adjusted for the blank. This data can be found on Table 1. These values are compared to the values produced by the model's Mout_1 and Mout_2 predictions for the Amite River watershed.

Table 1. October sampling results. List of sample sites with their predicted and observed plastic waste output values and flow measures.

Site Name	Date	Type	Micro-plastic (# m^{-3})	Macro-plastic (# m^{-3})	Micro-plastic (g m^{-3})	Macro-plastic (g m^{-3})	Total Plastic (g m^{-3})	Total Plastic (kg m^{-3})	Observed Output (observed - blank) (kg m^{-3})	Predicted Average Flow (m^3/month)
Pumpkin Patch Creek	10/23/20	Low	11.67	0.47	0.04	0.08	0.11	1.14E-04	2.58E-05	2538.78
Mill Creek	10/22/20	Low	26.67	1.07	0.08	0.18	0.26	2.61E-04	1.73E-04	1891.01
Days Creek	10/23/20	Medium	11.00	0.44	0.03	0.07	0.11	1.08E-04	1.98E-05	11164.83
Cotton Creek	10/23/20	Medium	11.67	0.47	0.04	0.08	0.11	1.14E-04	2.58E-05	2821.19
Bayou Barbery	10/20/20	High	32.00	1.28	0.10	0.22	0.31	3.14E-04	2.26E-04	749168.64
Clay Cut Bayou	10/21/20	High	14.33	0.57	0.04	0.10	0.14	1.40E-04	5.18E-05	238841.86

Table 2. November sampling results. List of sample sites with their predicted and observed plastic waste output values and flow measures. Bolded numbers indicate that the observed output after correcting for the blanks is a negative number.

November

Site Name	Date	Type	Micro-plastic (# m^{-3})	Macro-plastic (# m^{-3})	Micro-plastic (g m^{-3})	Macro-plastic (g m^{-3})	Total Plastic (g m^{-3})	Total Plastic (kg m^{-3})	Observed Output (observed - blank) (kg m^{-3})	Predicted Average Flow (m^3/month)
Pumpkin Patch Creek	11/15/2020	Low	8.00	0.32	0.02	0.05	0.08	7.84E-05	**-9.80E-06**	11163.42
Mill Creek	11/18/2020	Low	12.00	0.48	0.04	0.08	0.12	1.18E-04	2.98E-05	12891.01
Days Creek	11/15/2020	Medium	5.33	0.21	0.02	0.04	0.05	5.23E-05	**-3.59E-05**	60156.85
Cotton Creek	11/15/2020	Medium	55.00	2.20	0.17	0.37	0.54	5.39E-04	4.51E-04	14130.99
Bayou Barbery	11/17/2020	High	4.67	0.19	0.01	0.03	0.05	4.57E-05	**-4.25E-05**	3608308.54
Clay Cut Bayou	11/17/2020	High	10.67	0.43	0.03	0.07	0.10	1.05E-04	1.68E-05	1356286.27

Table 3. December sampling results. List of sample sites with their predicted and observed plastic waste output values and flow measures. Bolded numbers indicate that the observed output after correcting for the blanks is a negative number.

December

Site Name	Date	Type	Micro-plastic (# m^{-3})	Macro-plastic (# m^{-3})	Micro-plastic (g m^{-3})	Macro-plastic (g m^{-3})	Total Plastic (g m^{-3})	Total Plastic (kg m^{-3})	Observed Output (observed - blank) (kg m^{-3})	Predicted Average Flow (m^3/month)
Pumpkin Patch Creek	12/4/2020	Low	11.67	0.47	0.04	0.08	0.11	1.14E-04	2.58E-05	31666.64
Mill Creek	12/6/2020	Low	7.00	0.28	0.02	0.05	0.07	6.86E-05	**-1.96E-05**	22334.79
Days Creek	12/4/2020	Medium	21.67	0.87	0.07	0.15	0.21	2.12E-04	1.24E-04	144639.32
Cotton Creek	12/4/2020	Medium	25.67	1.03	0.08	0.17	0.25	2.52E-04	1.64E-04	35980.21
Bayou Barbery	12/5/2020	High	16.33	0.65	0.05	0.11	0.16	1.60E-04	7.18E-05	6497700.02
Clay Cut Bayou	12/5/2020	High	9.33	0.37	0.03	0.06	0.09	9.15E-05	3.30E-06	2568069.83

Any microparticles that were observed and looked similar to microplastics (but were not identified as microplastics) were listed in the 'other' category or were taken note of on the observation sheets. In addition, any tears in the filter used for the sample were noted in the observation sheets.

The observed outputs of all of the triplicates for all of the months were averaged together for all three months of sampling to generate one aggregate value and was compared to the predicted Mout_1 and Mout_2 outputs of the model to see if there were any increase of output in between the low, medium, and high outputs (Figures 8 and 9).

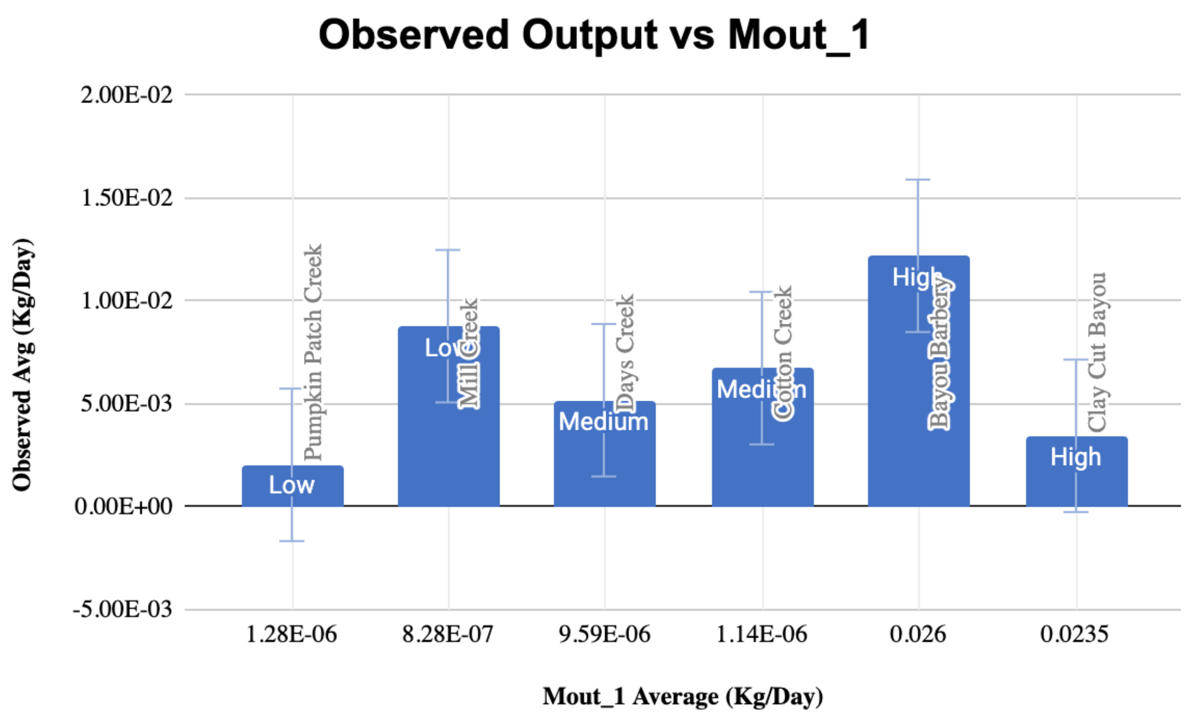

Figure 8. The averaged observed outputs in comparison to the Mout_1 predicted for the watersheds sampled. The error bars are the standard deviations of the observed values.

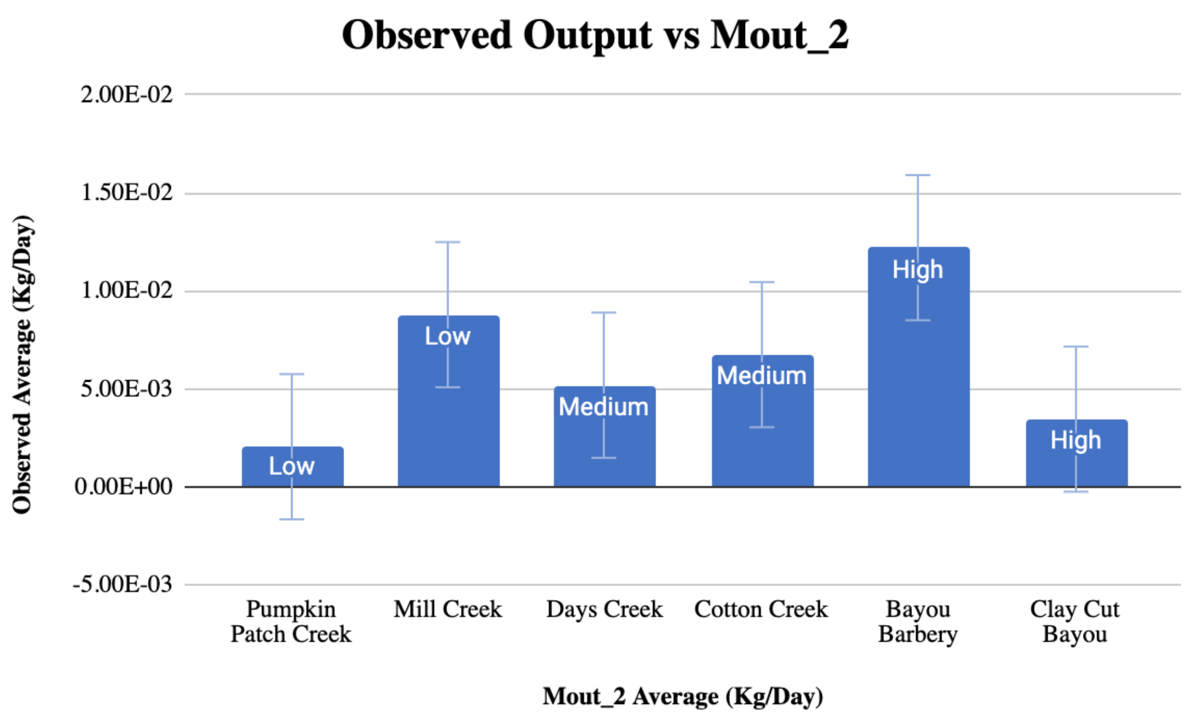

Figure 9. The averaged observed outputs in comparison to the Mout_2 predicted for the watersheds sampled at. The error bars are the standard deviations of the observed values.

The observed values' averages and Mout_1, and Mout_2 values are in the appendix. The site with the highest average observed output was Bayou Barbary, while the site with the lowest observed output was Mill Creek. Even though Mill Creek's observed output was small. All four of the low and medium output subwatersheds (Pumpkin Patch Creek, Mill Creek, Days Creek and Cotton Creek) far exceeded the Mout_1 and Mout_2 predictions from the model by several magnitudes. Bayou Barbery's output was of the same magnitude that was predicted by the Mout_2 from the model, while Clay Cut Bayou, the other high output subwatershed, was two magnitudes smaller than what was predicted by the model.

The observed outputs across the triplicate sampling periods and for all three months of sampling were averaged together and were compared to the Mout_1, Mout_2, runoff and populations for the sample site's watersheds using linear regressions. The results show that the individual sub-watershed contribution model (Mout_1) was not predictive of the observed in-situ

values (R^2 = 0.03, df = 16, p = 0.49, Figure 8). The cumulative model, Mout_2, was also not predictive of the observed plastic values (R^2 = 0.03, df = 16, p = 0.49, Figure 9). Runoff values were not predictive of the observed plastic values (R^2 = 1.03, df = 16, p = 0.85, Figure 10), and neither were the sub-watershed population estimates (R^2 = 1.023, df = 16, p = 0.63, Figure 11).

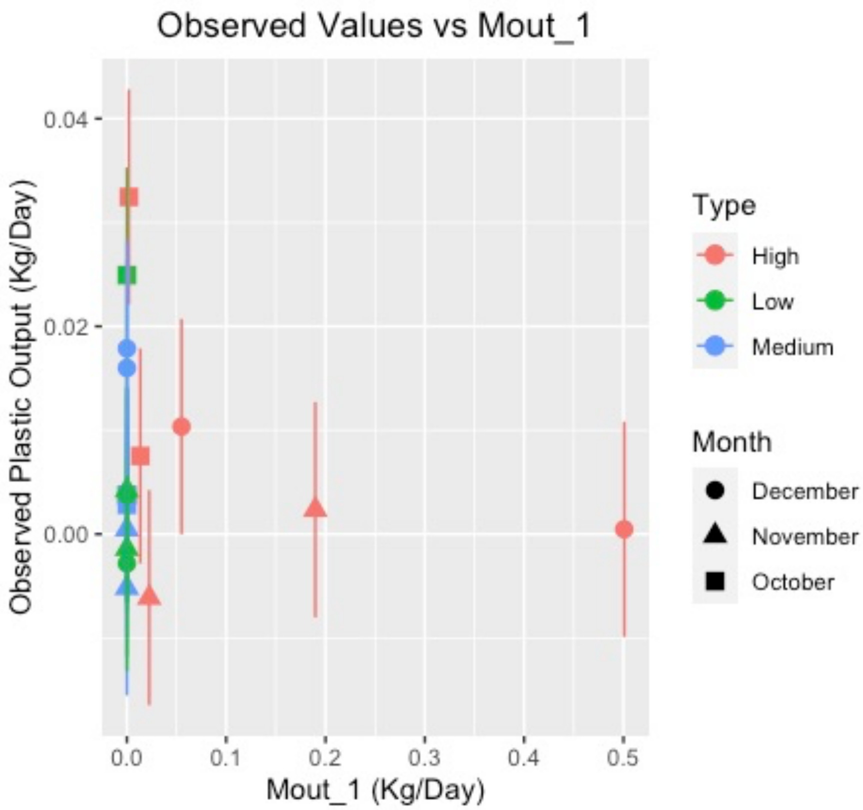

Figure 10. Observed values compared to the Mout_1 organized by sample month and sample subwatershed type.

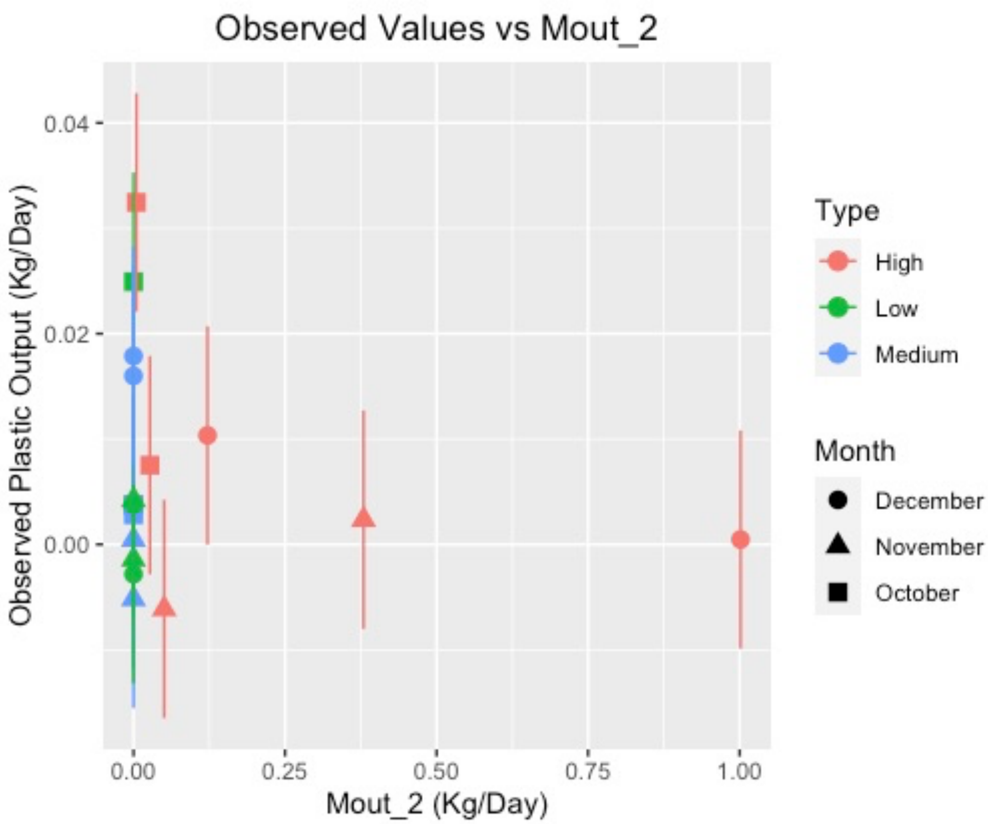

Figure 11. Observed values compared to the Mout_2 organized by sample month and sample subwatershed type.

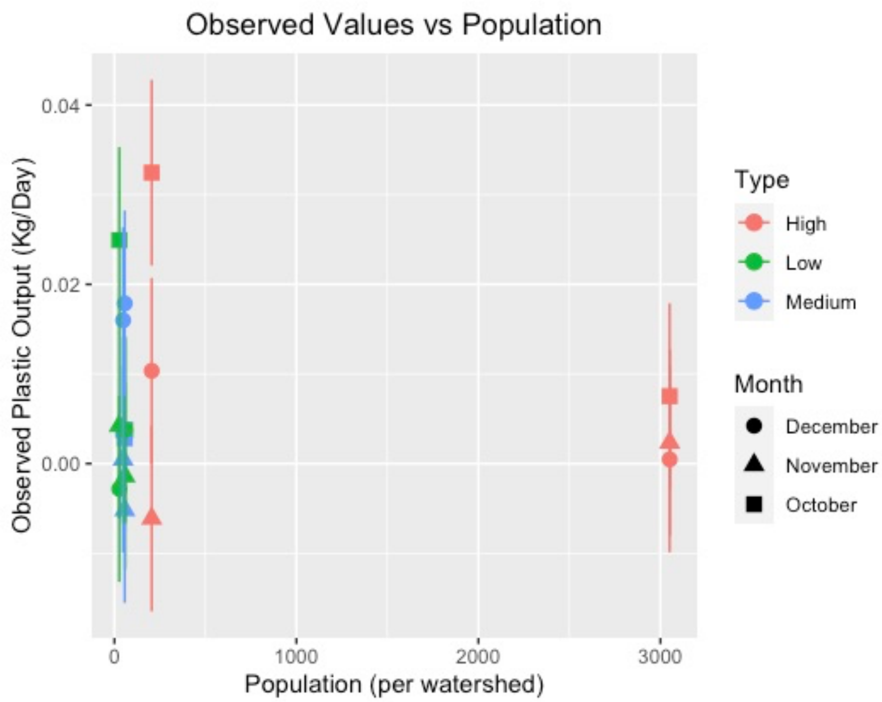

Figure 12. Observed values compared to the population of the sampled watersheds organized by sample month and sample subwatershed type.

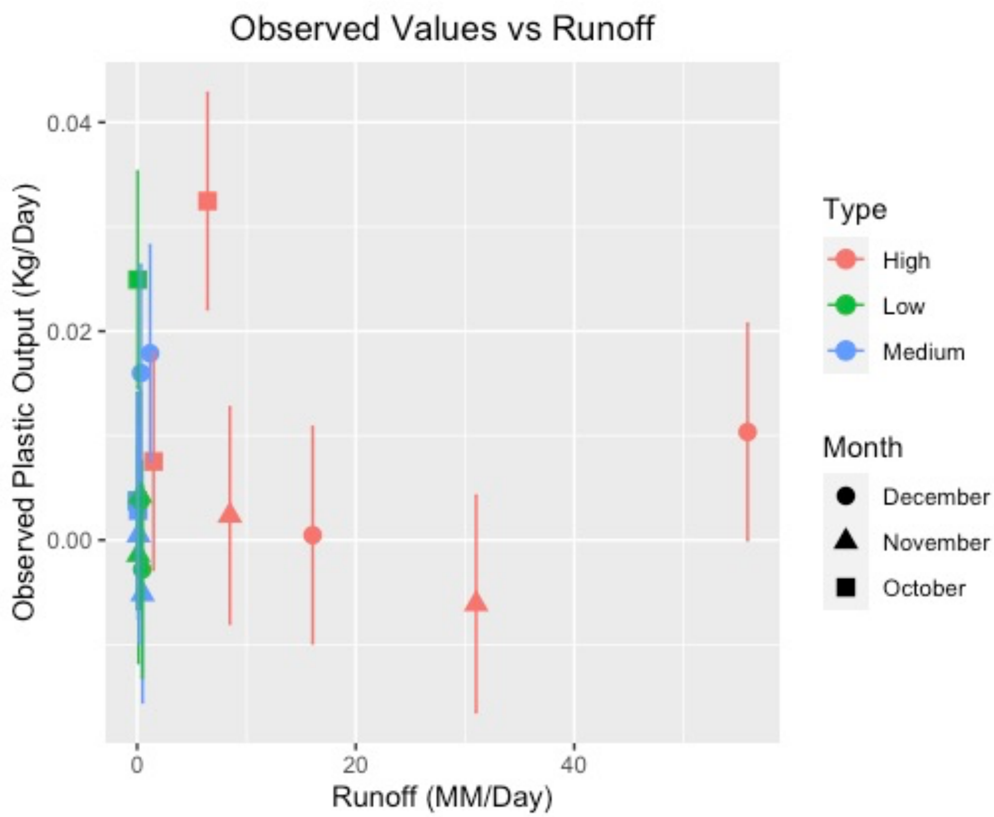

Figure 13. Observed values compared to the daily runoff of the sampled watersheds organized by sample month and sample subwatershed type.

A 2-Way ANOVA was conducted on the observed values with the sampling months and watershed type. The results show no significant relationship between the categories attributed to the sites based on model predictions (High, Medium, Low, Figure 12), and the observed plastic values (p-value = 0.06). Sampling month was also not predictive of the observed values (p-value = 0.88), and neither was the interaction between site type and sampling month (p-value = 0.19). This means that a trend was not able to be determined in between the sampling month, type of watershed sampled and the observed output.

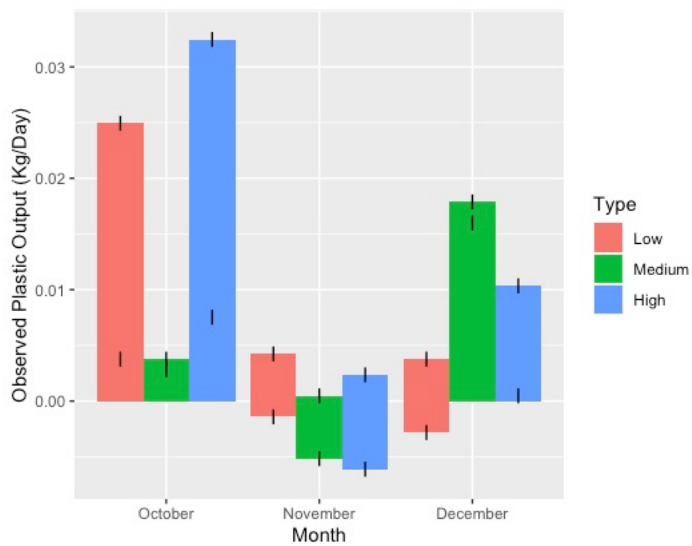

Figure 14. Average observed plastic output compared to the month of sampling, organized by sample site type. The error bars are fixed at the data points, and represent the standard deviation of the mean.

5. Discussion.

5.1. Discussion of the Model.

Figure 15. Clay Cut Bayou's sampling location.

This study adapted a previously created model for plastic waste output for coastal watershed, adjusting it to include inland watersheds at a finer spatial resolution and updated population density parameters. An in-situ component to the study as well, sampling at six different sampling sites at a gradient of plastic waste outputs (low, medium, and high) for three months to see whether observed plastic waste outputs match what the model predicted.

According to the model, the top four plastic pollution producing HUC-12 watersheds (Mout 1) are located on the west side and at the bottom of the Amite River, the first two, Manchac Point-Mississippi River and Claiborne Island-Mississippi River, being close to the Mississippi River and the latter two, Clay Cut Bayou-Amite River, and Bayou Barbery-Amite River, being close to Lake Maurepas, respectively. These four watersheds produce an estimated total of 6,593 kg of plastic per year and see 99.97% of the plastic waste to the aggregate total of all 81 watersheds found in the Amite River. These four watersheds also represent 6.06% of the total amount of area in the Amite River watershed.

In comparison with the four watersheds that had the highest predicted plastic loadings, the four watersheds with the lowest individual loadings (Mout_1) were Matthews Creek-Thompson Creek, West Branch Tickfaw River-Tickfaw River, Channey Creek-Darling Creek, and Goober Creek-McGehee Creek. These four watersheds contributed <0.01% of the plastic waste to the 81 watersheds and amounted to 4.38% of the total area in the Amite River watershed.

The Amite sub-watersheds' plastic output range from 2.76×10^{-7} kg/day at the smallest watershed (Goober Creek-McGehee Creek), to 406.76 kg/day at the largest watershed (Lake Maurepas). The Amite River's two tributaries are both at the head of the waterway in Mississippi, joining at the Mississippi and Louisiana state line. The East Fork tributary of the Amite River contributes 1.052×10^{-5} kg/day, while the West Fork tributary contributes 2.15×10^{-4} kg/day, making the East Fork tributary the main contributing waterway to the Amite River.

The model omits several land use features that may have been influential in plastic emissions. For future studies, the model should account for camping grounds, areas designated for hunting, fishing, and road density, usage and vehicle traffic surrounding the waterways that are being evaluated to improve model accuracy. Camping grounds, though can be seen as a way of protecting natural resources, can contribute to plastic waste output if the campsite is not carefully managed (Aikoh 2006). Fishing in marine environments' impacts on plastic waste pollution has been well documented, however, there is limited research done on what the impacts of terrestrial hunting areas have on plastic waste concentrations into freshwater environments (Deshpande 2020).

Road density and other roadway related objects (road marking paint and tire fragments from roads) have been known to contribute to microplastic waste, however, there are knowledge

gaps on direct quantities due to the complexities in their inputs and outputs into the environment (Horton et al. 2017, Kole et al. 2017). Traffic as well is estimated to be one of the largest sources of microplastics (Bondelind et al. 2018). Establishing a road traffic density map and integrating into a future model for plastic waste output would be immensely helpful. Camping, hunting, and road and vehicle related microplastic waste are independent of population density and runoff but can be affected by either one of those factors. Adding these factors to future models could assist in explaining as to why low population dense and low runoff areas can be observed to have more microplastics than initially expected.

5.2. Comparison to Other Studies.

For context, these results can be compared to those reported by Lebreton et al., (2017) for daily plastic outputs for the Tchefuncte watershed (the HUC-8 watershed adjacent to the Amite River watershed). The Tchefuncte watershed is roughly 1.6 times larger than the Amite watershed, at 1.37 x 10^{10} SqM as opposed to the Amite River's 8.25 x 10^{8} SqM total area. The runoff values that we estimated are along the lines of what was generated by Lebreton et al.'s model of the Tchefuncte watershed, ranging from 0.1 to 3 mm/day. Their plastic output predictions for the Tchefuncte watershed for the months of October, November, December are 0.18, 0.15 and 0.52 tons, respectively. The model conducted for the Amite River watershed's plastic waste output for the months of October, November, and December predicted 0.10, 0.30, and 0.72 tons, respectively. These outputs are similar in magnitude with what predicted by Lebreton et al.'s for the Tchefuncte River watershed for my three months of sampling, which suggests that my estimates yield plausible values, comparable to this previous study, and that my method can be replicated for other watersheds and sub-watersheds not previously assessed by Lebreton et al., (2017).

5.3. Discussion of the In-Situ Samples Results.

In-situ sampling results did not correlate to the model estimates, or the variables used as model inputs (runoff and population). Therefore, the estimates of the in-situ samples were not able to validate the estimates of this model through this study. The discrepancies found between the in-situ sampling and the model estimates may largely be due to the selected sampling approach. The sampling method described by in Kataoka et al 2019, which sampled their streams during consistently high flow conditions (enough to suspend their net at the surface of the water) and a depth deep enough to ensure that their sampling net was never able to touch the bottom of the waterway. On the other hand, the velocities of the flow at a majority of the sites were slow, making the flow readings inconsistent. The slow flow made it difficult to apply this method on the study sites, except during the month of December, where flow was faster due to recent rainfall events. This issue could have been partly the reason why we observed lower than expected values for the Clay Cut watershed, the highest predicted output site (Figures 13 and 14). Microplastics on this site may have been deposited on the bottom of the waterways more effectively than transported in the water column, and therefore the sampling approach may not have been able to capture true microplastic concentrations in this river.

In the future, sampling for microplastics in the slow-moving waters in Louisiana should be designed to integrate a variety of approaches, such as using a moving boat to create movement of flow and capture suspended particles (Barrows et al. 2017, Toner 2020), and sampling sediments (Besseling et al. 2017). Microplastics' sinking rates are linked to their shape, size, and density, along with several biotic factors such as water temperature and salinity (Kowalski et al. 2016). There is a direct relationship in between the velocity of sinking to a

particle's size, which means that larger particles would sink to the bottom of a waterway faster than smaller particles, which would be transported downstream. (Kowalski et al. 2016).

A higher-than-expected amount of plastic waste, seen in Figures 13 and 14, were observed in the samples at Mill Creek due to two suspected reasons. In certain occasions, the sample net and cod end touched the bottom at the waterway. This caused agitation of the benthic layer, resulting a large amount of sediment entering the net, unlike in the other sampling sites. The influx of sediment into the samples may have agitated and carried microplastics that were trapped in the benthic layer with it. Sediment layers at the bottom of waterways have been recognized to be sinks for larger, less mobile microplastic particles (Besseling et al. 2017), which could explain as to why we saw so many microplastic particles in the samples in Mill Creek. This is the only sample site that was shallow enough to cause this issue, but it highlights the importance of including sediment sampling into plastic estimates within river systems in the future, as this was the site with the highest observed plastic values.

5.4. Study Limitations

There were several limitations in this study. The timing of these sampling could have been a limiting factor for this study, as sampling took place after rain events at some sample sites and times but not for others, seen in Table 6 where the December sample's flow was much higher than the October and November's observed flows. This variability affected the flow of the watersheds, thus, the flow of the water moving through the nets, resulting in potentially less microplastics being collected in these water samples. Sampling was only conducted for three months out of the year, but if time permitted, a year's worth of sampling would have offered a more detailed study to match the years' worth of data from the model. However, a period with high rainfall was selected for sampling, and therefore the selected months should be an accurate

representation of the relative plastic concentrations across the watershed. In addition, we recommend sampling at the four highest waste producing watersheds (Manchac Point-Mississippi River, Claiborne Island-Mississippi River, Clay Cut Bayou-Amite River, and Bayou Barbery-Amite River). Though these watersheds cover a small area, they contribute most of the plastic pollution to the Amite River, and must be addressed in a future sampling and management plan accordingly. The management plan resulting from this model would be able to target point source microplastic sources in the Amite River watershed.

The sampling method chosen may have resulted in data bias. While Kataoka (and many others) conducted microplastic quantification studies in both marine and terrestrial waterways using plankton nets, it has been noted that the net itself could contribute microplastics to the sample (Kataoka et al. 2019, Sun et al. 2017, Barrows et al. 2017). While sampling off bridges with a plankton net is relatively safe, plastic particles from the net used fragmented off and interfered with the samples obtained. To account for this, blank samples were conducted. For future studies, it is advised to use alternative sampling methods to eliminate the risk of microplastic particles entering the sample from the sampling materials. Two alternatives to using plankton nets to collect samples would be to either use surface grabbing methods or sediment samples (Barrows et al. 2017, Scircle et al. 2020).

When treating and processing the samples, several additional limitations were encountered. Due to the ongoing COVID-19 pandemic, masks were mandated to be worn while sampling, treating, filtering and counting the samples. The masks, and clothes that were wore may have contaminated the resulting data - however, a precaution taken was to wear the same mask, lab jacket and outerwear during sampling, treatment, processing and counting procedures. The limitation of potential pollution of the samples with microplastics from these sources

(clothes, masks, etc) was accounted for by having sample blanks. The average microplastic value from the blanks was used to correct for the sample's observed mass. Optical microscopy was used to count the microplastics in the samples. Though Raman spectroscopy and gas chromatography/mass spectrometry have been proven to give the most accurate results in between particle number and polymer type, microscopy is the best at quantifying the total plastic particle numbers, which was the goal for the on-site microplastic sampling (Müller et al. 2019). For future analyses, Fourier-transform infrared spectroscopy (FTIR) is recommended to be used to analyze particles in samples. That method is widely available and would provide for accurate particle analysis to determine whether particles are plastic or not.

Lastly, study sites chosen were limited in number due to the procedure chosen and the timeframe of sampling was relatively short. Sampling at a greater number of sites and using repeated measures through time, would allow for a complete and cohesive data collection survey, for validating the predictive model. In spite of these limitations, partial validation for this modelling approach was observed with 4 of the 6 sites showing the expected trend. For the other two sites, potential reasons for having different than expected results were defined, those issues can be better corrected for with in-situ sampling procedures that better reflect slow moving rivers for lowland sites, and modelling that considers other potential sources of pollution aside from population density.

6. Conclusion

This study developed an approach for estimating plastic outputs from HUC-12 watersheds, based on existing models at larger, coarser spatial resolutions. The model's estimates can be used as a baseline for developing validation projects and monitoring efforts in the Amite River. The model's process can be replicated in the future for studies focusing on tributaries or sub watershed of larger river systems. Nevertheless, the attempt to validate this modelling method in the Amite watershed with in-situ sampling was not effective resulting in discrepancies with the predicted model. Therefore, future studies should focus on validating this model through other sampling procedures. For future studies in the Amite watershed, using methods that account for low flow and sediment-microplastic loads, instead of plankton nets which solely account for surface water microplastics, would be recommended, due to the slow-moving nature of its waterways. For modelling purposes, incorporating other landscape usage indicators, such as locations for recreational activities (camping, hunting, fishing), and road density, could potentially help improve the predictions for microplastic exports, and should also be considered.

Appendix A. How to recreate study

You need HUC-12 watersheds, EROM runoff files for every month, blockgroup population files, and a layer indicating where dams are located.

- HUC-12 Shapefiles were obtained from the USGS website.
- EROM runoff files were obtained from National Hydrgraphy Dataset
- GRASP population files were found on the Center for Disease Control (CDC) website.
- Dam layer was obtained from National Hydrgraphy Dataset

1. Calculate the areas of the HUC12 watersheds
    a. Add new field (field type: double, name: areasqm), and use the calculate areas tool to determine the areas in sqm.
2. Merge the population file with the HUC12 watershed shapefile.
    a. Select the identity tool, and use the GRASP population and the HUC12 shapefile as your input features.
    b. Join based off HUC12 using the mean.
3. Calculate the Mmpw of each watershed
    a. Create a new field (field type double) and multiple the population value by the mismanaged waste value in the US (0.007 kg/person/day)
4. Calculate the runoff at the HUC12 watersheds
    a. Concert all of the EROM files from polygon to raster (polygon to raster function), value field will be Q0001A.
        i. Horizontal and vertical resolution should be 5000 x 5000.
        ii. Save as TIF file.
    b. Conduct zonal statistics by table, using HUC12 as the zone, statistics type is all. Name each file by the month of the runoff.
    c. Convert the average runoff from CFS/day to MM/day
        i. Multiply original value by 0.028316847
        ii. Multiply that value by 86400 (seconds per day)
        iii. Divide by HUC12 area in m2
        iv. Multiply that value by 1000 to get mm/day per HUC12 watershed.
5. Add dam layer to see if there are any dams that fall within the study area.
6. Identify dams in watershed
    a. Select by target
    b. Target layer HUC12
    c. Source layer dams
    d. Spatial selection method
    e. Intersect the source layer or contain the source layer
    f. Create a new field in the attribute table (field type double) and name it Dams
    g. Right click this field and click on the field calculator.

        i. Put the number 1 on this box, all of the HUC12 watersheds that have a dam in them will have a 1 in this box, if not, it will have a 0.

7. Calculate the Mout1
    a. $$M_{\text{out}} = \left(kM_{\text{mpw}}R\right)^{a}, \qquad (1)$$
    b. K = 1.85*10^-3
    c. R = Runoff calculated by month from erom raster, in mm/day
    d. A = 1.52
8. Identify HUC12s influenced by other HUC12s' populations
    a. Dissolve the union of the HUC12 shapefiles, use the summarize function the population estimates by the attribute ToHUC.
        i. The output will be the sum of the watersheds that drain to the listed watersheds
    b. Join the output table to the HUC12 shapefile by HUC12.
9. Summarize population by ToHuc
    a. Right click on the attribute ToHUC, click summarize. Select the population and choose sum
        i. Output will be the sum of population from all of the watersheds drained into this watershed
    b. Create a new field called TotPop (field type double)
        i. Click on the field calculator and do a sum of the ToHuc population + the original population
        ii. Multiple this new population by 0.007 kg/person/day to get the new Mmpw
10. Identify HUC12's influenced by other HUC12's runoff.
    a. Dissolve the union of the HUC12 shapefiles, use the summarize function by the runoff values, attribute ToHUC.
        i. The output will be the sum of the watersheds that drain to the listed watersheds
    a. Join the output table to the HUC12 shapefile by HUC12.
    b. Calculate the Mout_2 using the same equation as above using the new values for the population and runoff.

Appendix B. Output of Model for all of the Subwatersheds of the Amite River Watershed (Table 4)

HUC12 Code	HUC12 Watershed Name	ToHUC	Dams	Population (per watershed)	Area (SqM)	Mmpw (Kg/Person/Day)	Mout_1 (Kg/Year)	Mout_1 (Kg/Day)	Mout_2 (Kg/Year)	Mout_2 (Kg/Day)
80702030401	Wall Bayou-Tickfaw River	80702030403	0	1.39E+02	9.49E+07	9.73E-01	5.27E-03	1.45E-05	2.84E-01	7.78E-04
80702030403	Killian Bayou-Tickfaw River	80702040400	0	1.39E+02	6.91E+07	9.73E-01	6.44E-02	1.76E-04	1.69E+01	4.64E-02
80702040102	Black Bayou-Saveiro Canal	80702040103	0	1.21E+03	7.79E+07	8.46E+00	3.08E-03	8.43E-06	1.69E-01	4.63E-04
80702040103	Grand Goudine Bayou-New River	80702040104	0	6.20E+02	7.14E+07	4.34E+00	2.86E-02	7.85E-05	1.57E+00	4.31E-03
80702040104	Bayou Pierre-Petite Amite River	80702040204	0	2.88E+02	9.29E+07	2.02E+00	2.70E-03	7.40E-06	1.48E-01	4.07E-04
80702040205	Bayou Chene Blanc-Blind River	80702040400	0	1.36E+02	1.31E+08	9.52E-01	3.76E-02	1.03E-04	1.62E+01	4.44E-02
80702040400	Lake Maurepas	80702040504	0	7.00E+00	2.43E+08	4.90E-02	5.47E-04	1.50E-06	2.96E-02	8.12E-05
80702010301	Matthews Creek-Thompson Creek	80702010302	0	3.30E+01	1.07E+08	2.31E-01	8.00E-06	2.19E-08	4.26E-04	1.17E-06
80702010302	Lost Creek-Thompson Creek	80702010303	0	1.20E+02	8.35E+07	8.40E-01	6.71E-05	1.84E-07	3.60E-03	9.87E-06
80702020106	Cars Creek-East Fork Amite River	80702020401	0	3.70E+01	1.42E+08	2.59E-01	2.47E-04	6.76E-07	2.36E-02	6.46E-05
80702020205	Mill Creek-West Fork Amite River	80702020401	0	2.80E+01	1.05E+08	1.96E-01	3.42E-04	9.38E-07	2.61E-02	7.16E-05
80702020303	Outlet Beaver Creek	80702020401	0	4.70E+01	1.05E+08	3.29E-01	5.18E-05	1.42E-07	1.84E-02	5.04E-05
80702020401	Clear Creek-Amite River	80702020405	0	6.70E+01	1.37E+08	4.69E-01	1.50E-03	4.10E-06	8.13E-02	2.23E-04
80702020402	Channey Creek-Darling Creek	80702020403	0	2.00E+01	7.59E+07	1.40E-01	5.23E-06	1.43E-08	2.81E-04	7.69E-07
80702020601	Little Comite Creek	80702020603	0	5.20E+01	5.71E+07	3.64E-01	6.02E-05	1.65E-07	4.96E-03	1.36E-05
80702020602	Richland Creek-Comite Creek	80702020603	0	9.70E+01	9.88E+07	6.79E-01	6.50E-05	1.78E-07	5.08E-03	1.39E-05
80702030102	Cuba Creek-Tickfaw River	80702030103	0	2.50E+01	9.62E+07	1.75E-01	9.06E-06	2.48E-08	4.82E-04	1.32E-06
80701000104	Manchac Point-Mississippi River	80701000105	0	2.47E+02	6.82E+07	1.73E+00	4.89E+03	1.34E+01	2.57E+05	7.05E+02

80701000105	Claiborne Island-Mississippi River	80901000101	0	2.43E+02	1.56E+08	1.70E+00	1.69E+03	4.64E+00	8.90E+04	2.44E+02
80702010303	Beaver Creek-Thompson Creek	80702010306	0	1.79E+02	6.70E+07	1.25E+00	7.94E-04	2.17E-06	4.26E-02	1.17E-04
80702010306	Hammer Creek-Thompson Creek	80702010308	0	5.47E+02	1.09E+08	3.83E+00	3.64E-02	9.96E-05	1.95E+00	5.35E-03
80702010308	Sandy Creek-Thompson Creek	80701000103	0	3.47E+02	1.06E+08	2.43E+00	4.17E-02	1.14E-04	3.29E+00	9.00E-03
80702010401	Cypress Bayou-Bayou Baton Rouge	80702010402	0	1.04E+03	1.58E+08	7.30E+00	1.40E-03	3.84E-06	7.62E-02	2.09E-04
80702010402	Devils Swamp-Bayou Baton Rouge	80701000103	0	1.97E+03	7.01E+07	1.38E+01	3.81E-02	1.04E-04	3.21E+00	8.78E-03
80702020403	Sandy Run-Darling Creek	80702020405	0	4.30E+01	9.99E+07	3.01E-01	5.02E-05	1.38E-07	4.28E-02	1.17E-04
80702020404	Bluff Creek	80702020405	0	4.50E+01	7.40E+07	3.15E-01	1.06E-05	2.90E-08	4.17E-02	1.14E-04
80702020405	Pigeon Creek-Amite River	80702020406	0	9.40E+01	1.48E+08	6.58E-01	1.57E-03	4.30E-06	8.38E-02	2.29E-04
80702020406	Kidds Creek-Amite River	80702020902	0	2.13E+02	1.21E+08	1.49E+00	6.37E-02	1.75E-04	1.27E+01	3.48E-02
80702020501	Hunter Bayou-Sandy Creek	80702020504	0	7.40E+01	1.08E+08	5.18E-01	9.37E-06	2.57E-08	7.48E-03	2.05E-05
80702020502	Mill Creek	80702020504	0	2.70E+01	4.87E+07	1.89E-01	1.45E-05	3.98E-08	7.62E-03	2.09E-05
80702020503	Little Sandy Creek	80702020504	0	1.25E+02	7.64E+07	8.75E-01	2.43E-04	6.65E-07	1.38E-02	3.78E-05
80702020504	Beaver Pond Bayou-Sandy Creek	80702020902	0	6.50E+01	6.57E+07	4.55E-01	9.34E-04	2.56E-06	1.10E+01	3.02E-02
80702020603	Pretty Creek-Comite River	80702020604	0	1.70E+02	1.42E+08	1.19E+00	3.50E-04	9.60E-07	1.88E-02	5.15E-05
80702020604	Knighton Bayou-Comite River	80702020607	0	2.86E+02	1.34E+08	2.00E+00	7.29E-03	2.00E-05	4.39E-01	1.20E-03
80702020605	Doyle Bayou-Redwood Creek	80702020607	0	3.41E+02	1.56E+08	2.39E+00	3.95E-04	1.08E-06	2.54E-01	6.95E-04
80702020606	White Bayou	80702020607	0	9.35E+02	1.44E+08	6.55E+00	1.33E-03	3.64E-06	2.79E-01	7.64E-04
80702020607	Blackwater Bayou-Comite River	80702020608	0	5.12E+02	8.92E+07	3.58E+00	1.28E-02	3.51E-05	6.93E-01	1.90E-03
80702020608	Hurricane Creek-Comite River	80702020902	0	3.89E+03	1.62E+08	2.72E+01	3.43E-01	9.39E-04	2.03E+01	5.55E-02
80702020701	Hornsby Creek-Colyell Creek	80702020704	0	3.98E+02	1.10E+08	2.79E+00	4.81E-04	1.32E-06	8.71E-02	2.39E-04
80702020702	West Colyell Creek	80702020703	0	9.96E+02	1.14E+08	6.97E+00	5.58E-03	1.53E-05	3.04E-01	8.32E-04
80702020703	Middle Colyell Creek	80702020704	0	5.41E+02	1.10E+08	3.79E+00	2.24E-03	6.15E-06	1.35E-01	3.70E-04
80702020704	Little Colyell Creek-Colyell Creek	80702020904	0	4.19E+02	1.37E+08	2.93E+00	1.64E-03	4.50E-06	1.33E+01	3.65E-02
80702020801	Bayou Braud	80702020802	0	1.99E+02	5.60E+07	1.39E+00	5.96E-04	1.63E-06	3.25E-02	8.92E-05
80702020802	Alligator Bayou-Bayou Braud	80702020804	0	1.16E+03	1.11E+08	8.09E+00	4.11E-03	1.13E-05	2.54E+00	6.96E-03
80702020803	Ward Creek	80702020804	0	7.50E+03	1.17E+08	5.25E+01	8.44E-02	2.31E-04	4.75E+00	1.30E-02

80702020804	Bayou Fountain-Bayou Manchac	80702020904	0	3.47E+03	1.53E+08	2.43E+01	3.76E-02	1.03E-04	1.43E+01	3.92E-02
80702020901	Jones Creek	80702020904	0	3.63E+03	6.28E+07	2.54E+01	4.25E-02	1.16E-04	1.44E+01	3.96E-02
80702020902	Beaver Creek-Amite River	80702020904	0	1.29E+03	9.85E+07	9.00E+00	4.09E-01	1.12E-03	2.42E+01	6.64E-02
80702020903	Grays Creek	80702020904	0	8.45E+02	8.83E+07	5.92E+00	2.90E-03	7.95E-06	1.34E+01	3.66E-02
80702020904	Clay Cut Bayou-Amite River	80702020905	0	3.05E+03	1.60E+08	2.14E+01	4.26E+00	1.17E-02	2.29E+02	6.28E-01
80702020905	King George Bayou-Amite River	80702020906	0	1.67E+02	8.07E+07	1.17E+00	9.77E-02	2.68E-04	5.27E+00	1.44E-02
80702020906	Bayou Barbary-Amite River	80702040400	0	2.05E+02	1.16E+08	1.44E+00	4.61E-01	1.26E-03	2.76E+01	7.57E-02
80702030103	Crittenden Creek-Tickfaw River	80702030105	0	8.90E+01	1.22E+08	6.23E-01	2.06E-04	5.64E-07	1.38E-02	3.79E-05
80702030104	Twelvemile Creek	80702030105	0	1.08E+02	1.19E+08	7.56E-01	1.06E-04	2.90E-07	1.12E-02	3.07E-05
80702030105	Joseph Branch-Tickfaw River	80702030205	0	1.08E+02	1.18E+08	7.56E-01	8.96E-04	2.46E-06	4.54E-01	1.24E-03
80702030201	Beaver Dam Creek	80702030202	0	2.80E+01	4.80E+07	1.96E-01	3.46E-05	9.48E-08	1.88E-03	5.14E-06
80702030202	West Hog Branch	80702030204	0	7.80E+01	1.03E+08	5.46E-01	5.56E-05	1.52E-07	3.01E-03	8.24E-06
80702030204	Beaver Pond Branch-Hog Branch	80702030205	0	1.51E+02	4.85E+07	1.06E+00	1.50E-02	4.11E-05	8.35E-01	2.29E-03
80602050201	Headwaters McGehee Creek	80602050202	0	1.40E+01	4.20E+07	9.80E-02	1.04E-05	2.84E-08	5.48E-04	1.50E-06
80602050202	Goober Creek-McGehee Creek	80602050203	0	1.70E+01	6.59E+07	1.19E-01	3.33E-06	9.14E-09	1.76E-04	4.82E-07
80602050306	Wolvington Branch-Porter Creek	80602050307	0	1.10E+01	4.12E+07	7.70E-02	8.97E-06	2.46E-08	4.72E-04	1.29E-06
80602050501	Middleton Creek	80602050503	0	2.30E+01	7.25E+07	1.61E-01	1.31E-05	3.58E-08	9.44E-04	2.59E-06
80602050502	Caston Creek	80602050503	0	1.30E+01	4.44E+07	9.10E-02	9.56E-06	2.62E-08	8.52E-04	2.33E-06
80602050504	Birdman Branch-Brushy Creek	80602050507	0	3.00E+01	1.04E+08	2.10E-01	9.84E-06	2.69E-08	5.23E-04	1.43E-06
80602060101	Smith Creek-Buffalo River	80602060102	0	1.29E+02	8.89E+07	9.03E-01	1.62E-04	4.44E-07	8.62E-03	2.36E-05
80602060103	Little Buffalo River	80602060106	0	4.00E+01	9.16E+07	2.80E-01	2.08E-05	5.70E-08	1.11E-03	3.04E-06
80702020101	Pumpkin Patch Creek-East Fork Amite River	80702020102	0	5.90E+01	1.01E+08	4.13E-01	2.85E-05	7.80E-08	1.50E-03	4.12E-06
80702020102	Gordon Creek-East Fork Amite River	80702020103	0	6.20E+01	1.23E+08	4.34E-01	5.49E-05	1.51E-07	2.90E-03	7.95E-06
80702020103	Robinson Creek-East Fork Amite River	80702020105	0	4.30E+01	8.61E+07	3.01E-01	1.89E-05	5.17E-08	1.71E-03	4.69E-06
80702020104	Hominy Creek	80702020105	0	3.50E+01	9.03E+07	2.45E-01	2.69E-05	7.37E-08	1.92E-03	5.25E-06
80702020105	Love Creek-East Fork Amite River	80702020106	0	6.20E+01	7.04E+07	4.34E-01	2.48E-05	6.79E-08	1.32E-03	3.61E-06

80702020201	Cotton Creek-West Fork Amite River	80702020202	0	4.80E+01	1.03E+08	3.36E-01	2.38E-05	6.52E-08	1.26E-03	3.45E-06
80702020202	Days Creek-West Fork Amite River	80702020203	0	5.70E+01	1.22E+08	3.99E-01	1.95E-04	5.34E-07	1.03E-02	2.83E-05
80702020203	Speculation Creek-West Fork Amite River	80702020205	0	1.52E+02	8.73E+07	1.06E+00	2.04E-03	5.58E-06	1.09E-01	2.97E-04
80702020204	Waggoner Creek	80702020205	0	2.30E+01	7.36E+07	1.61E-01	1.36E-05	3.72E-08	5.48E-02	1.50E-04
80702020301	Little Beaver Creek-Beaver Creek	80702020302	0	1.44E+02	1.30E+08	1.01E+00	1.77E-04	4.86E-07	9.45E-03	2.59E-05
80702020302	Centreville Creek-Beaver Creek	80702020303	0	4.40E+01	8.77E+07	3.08E-01	9.19E-05	2.52E-07	4.90E-03	1.34E-05
80702030101	West Branch Tickfaw River-Tickfaw River	80702030102	0	2.40E+01	1.13E+08	1.68E-01	5.58E-06	1.53E-08	2.95E-04	8.09E-07
80702050101	Haymans Creek-Tangipahoa River	80702050102	0	1.27E+02	1.06E+08	8.89E-01	8.52E-05	2.33E-07	4.48E-03	1.23E-05
80702050102	Hurricane Creek-Tangipahoa River	80702050104	0	1.59E+02	1.01E+08	1.11E+00	7.30E-04	2.00E-06	3.82E-02	1.05E-04
31800050103	Sassers Mill Creek-Big Creek	31800050104	0	1.29E+02	1.44E+08	9.03E-01	7.20E-05	1.97E-07	3.81E-03	1.04E-05

Appendix C. Averaged Observed Outputs vs Predicted Outputs (Table 5)

Site	Type	Mout1 Avg (Kg/Day)	Mout2 Avg (Kg/Day)	Observed (Kg/Day)
Pumpkin Patch Creek	Low	1.28E-06	2.55E-06	2.04E-03
Mill Creek	Low	8.28E-07	1.18E-05	8.78E-03
Days Creek	Medium	9.59E-06	1.92E-05	5.18E-03
Cotton Creek	Medium	1.14E-06	2.27E-06	6.74E-03
Bayou Barbery	High	0.026	5.90E-02	1.22E-02
Clay Cut Bayou	High	0.0235	4.69E-01	3.45E-03

Appendix D. Observed Output vs Predicted Output (Table 6)

- The yellow highlighted cells indicate a less-than-zero number calculated after adjusting the observed output for the blank's average mass.

October

Site Name	Date	Low/Mid/High	Microplastic #	Macroplastic #	Microplastic g	Macroplastic g	Total Plastic g	Total Plastic kg	Observed Output (observed - blank) (kg)	Measured Flow (m^3/10 minutes)	Observed Plastic Output (kg/day)	Predicted Plastic Output (Mout_1) (kg/day)	Predicted Plastic Output (Mout_2) (kg/day)	Predicted Average Flow (m^3/month)
Pumpkin Patch Creek	10/23/2020	L	11.67	0.47	0.04	0.08	0.11	1.14E-04	2.58E-05	60.79	3.72E-03	6.73E-08	1.35E-07	2538.78
Mill Creek	10/22/2020	L	26.67	1.07	0.08	0.18	0.26	2.61E-04	1.73E-04	86.11	2.49E-02	4.24E-08	9.14E-07	1891.01
Days Creek	10/23/2020	M	11	0.44	0.03	0.07	0.11	1.08E-04	1.98E-05	47.62	2.85E-03	4.57E-07	9.13E-07	11164.83
Cotton Creek	10/23/2020	M	11.67	0.47	0.04	0.08	0.11	1.14E-04	2.58E-05	59.77	3.72E-03	5.64E-08	1.13E-07	2821.19
Bayou Barbery	10/20/2020	H	32	1.28	0.10	0.22	0.31	3.14E-04	2.26E-04	140.82	3.25E-02	2.06E-03	4.73E-03	749168.64
Clay Cut Bayou	10/21/2020	H	14.33	0.57	0.04	0.10	0.14	1.40E-04	5.18E-05	65.85	7.46E-03	1.35E-02	2.71E-02	238841.86

November

Site Name	Date	Low/Mid/High	Microplastic #	Macroplastic #	Microplastic g	Macroplastic g	Total Plastic g	Total Plastic kg	Total MP kg/10 mins - Blank kg	Measured Flow (m^3/10 minutes)	Observed Plastic Output (kg/day)	Predicted Plastic Output (Mout_1) (kg/day)	Predicted Plastic Output (Mout_2) (kg/day)	Predicted Average Flow (m^3/month)
Pumpkin Patch Creek	11/15/2020	L	8	0.32	0.02	0.05	0.08	7.84E-05	-9.80E-06	75.98	-1.41E-03	6.39E-07	1.28E-06	11163.42
Mill Creek	11/18/2020	L	12	0.48	0.04	0.08	0.12	1.18E-04	2.98E-05	1061.72	4.29E-03	7.39E-07	1.47E-05	12891.01
Days Creek	11/15/2020	M	5.33	0.21	0.02	0.04	0.05	5.23E-05	-3.59E-05	44.58	-5.17E-03	5.91E-06	1.18E-05	60156.85
Cotton Creek	11/15/2020	M	55	2.20	0.17	0.37	0.54	5.39E-04	4.51E-04	1013.09	6.49E-02	6.53E-07	1.31E-06	14130.99
Bayou Barbery	11/17/2020	H	4.67	0.19	0.01	0.03	0.05	4.57E-05	-4.25E-05	125.62	-6.12E-03	2.25E-02	5.06E-02	3608308.54
Clay Cut Bayou	11/17/2020	H	10.67	0.43	0.03	0.07	0.10	1.05E-04	1.68E-05	82.06	2.42E-03	1.90E-01	3.80E-01	1356286.27

December

Site Name	Date	Low/Mid/High	Microplastic #	Macroplastic #	Microplastic g	Macroplastic g	Total Plastic g	Total Plastic kg	Total MP kg/10 mins - Blank kg	Measured Flow (m^3/10 minutes)	Observed Plastic Output (kg/day)	Predicted Plastic Output (Mout_1) (kg/day)	Predicted Plastic Output (Mout_2) (kg/day)	Predicted Average Flow (m^3/month)
Pumpkin Patch Creek	12/4/2020	L	11.67	0.47	0.04	0.08	0.11	1.14E-04	2.58E-05	13870.20	3.72E-03	3.12E-06	6.24E-06	31666.64
Mill Creek	12/6/2020	L	7	0.28	0.02	0.05	0.07	6.86E-05	-1.96E-05	16.21	-2.82E-03	1.70E-06	3.38E-05	22334.79
Days Creek	12/4/2020	M	21.67	0.87	0.07	0.15	0.21	2.12E-04	1.24E-04	6037.00	1.79E-02	2.24E-05	4.48E-05	144639.32
Cotton Creek	12/4/2020	M	25.67	1.03	0.08	0.17	0.25	2.52E-04	1.64E-04	245.17	2.36E-02	2.70E-06	5.41E-06	35980.21
Bayou Barbery	12/5/2020	H	16.33	0.65	0.05	0.11	0.16	1.60E-04	7.18E-05	74.97	1.03E-02	5.50E-02	1.22E-01	6497700.02
Clay Cut Bayou	12/5/2020	H	9.33	0.37	0.03	0.06	0.09	9.15E-05	3.30E-06	13.17	4.75E-04	5.01E-01	1.00E+00	2568069.83

Appendix E. Runoff Averages at Grouped Sample Sites (Table 7)

Sample Sites (grouped)	**Month**	**Average Weekly Runoff (mm/day)**
Bayou Barbary/Clay Cut Bayou	October	4.06
Mill Creek	October	4.06
Pumpkin Patch/Cotton Creek/Days Creek	October	4.06
Bayou Barbary/Clay Cut Bayou	November	0.00
Mill Creek	November	0.00
Pumpkin Patch/Cotton Creek/Days Creek	November	0.00
Bayou Barbary/Clay Cut Bayou	December	4.06
Mill Creek	December	4.57
Pumpkin Patch/Cotton Creek/Days Creek	December	4.32

Appendix F. Amite River Discharge throughout the Sampling Period (Figure 16)

- The days sampling sessions occurred on are displayed as purple circles on the graph.

Discharge, cubic feet per second

Most recent instantaneous value: 3890 05-17-2021 09:15 CDT

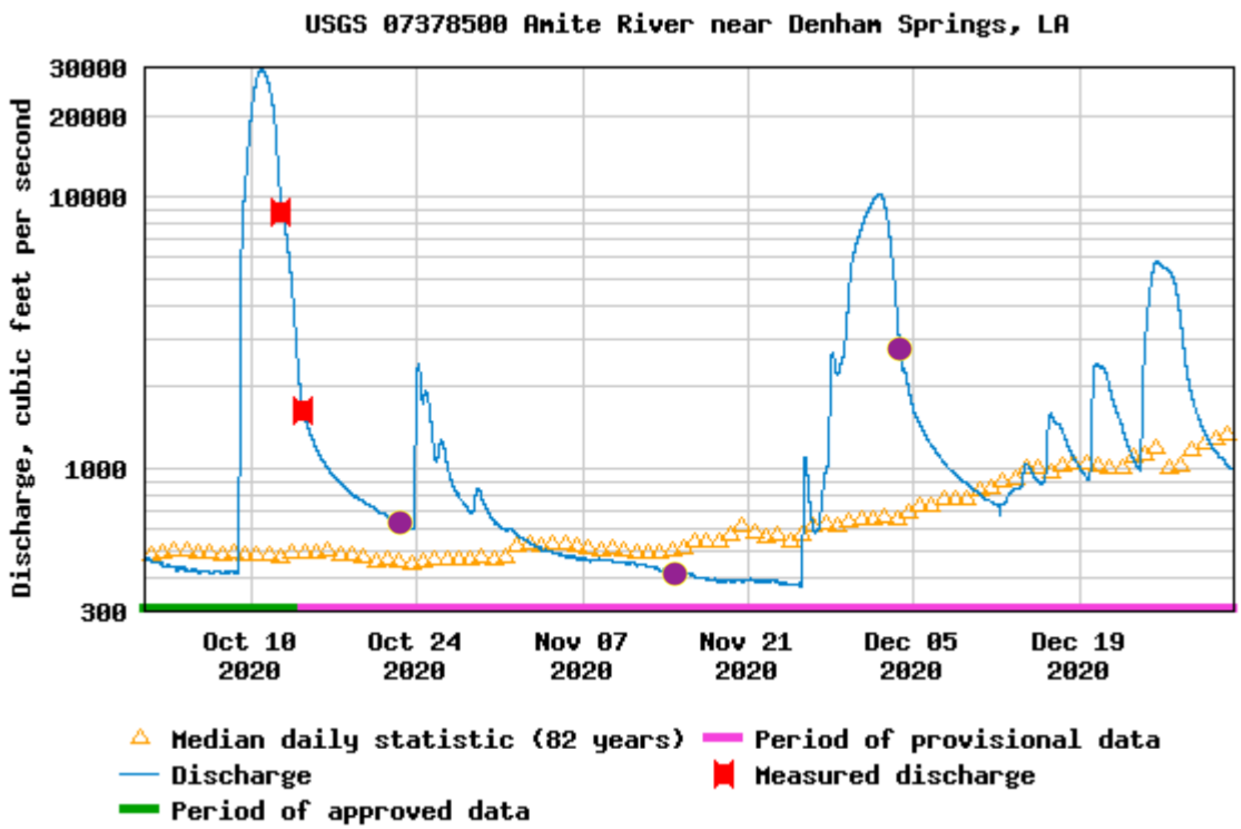

Source: U.S. Geological Survey, 2021, USGS 07378500 Amite River Discharge, accessed May 17, 2021 at URL https://waterdata.usgs.gov/usa/nwis/uv?site_no=07378500

Appendix G. Code for Statistical Analysis (for R)

```
setwd("~/Documents/MSThesis")
packages <- c("psych", "plotly", "plyr", "reshape2", "tidyverse", "ggpubr", "rstatix", "mvnormtest")
ipak(packages)
TStats2 <- read.csv("ThesisStatsRound2.csv", header=TRUE, sep=",")
View(TStats2)
TStats2 <- TStats2[-c(19,20,21,22,23,24,25,26), ]
TStats2 <- subset(TStats2, select=-c(X,X.1,X.2))
library(ggplot2)
library(tidyverse)
library(ggpubr)
library(rstatix)
sdob = sd(TStats2$ObsAdj)
limits <- aes(ymax = ObsAdj + sdob, ymin=ObsAdj-sdob)

Scaled_Observed<-scale(TStats2$ObsAdj, center=TRUE, scale = TRUE)
Scaled_Mout1<-scale(TStats2$Mout1, center=TRUE, scale = TRUE)
Scaled_Mout2<-scale(TStats2$Mout2, center=TRUE, scale = TRUE)
Scaled_Runoff<-scale(TStats2$Runoff, center=TRUE, scale = TRUE)
Scaled_Pop<-scale(TStats2$Population, center=TRUE, scale = TRUE)

sd_scaledob = sd(Scaled_Observed)
limits_sc <- aes(ymax = Scaled_Observed + sd_scaledob, ymin=Scaled_Observed-sd_scaledob)

## Linear regression of observed vs Mout1
require(stats)
reg <- lm(ObsAdj ~ Mout1, data=TStats2)
reg
summary(reg)
ggplot(TStats2, aes(x=Mout1, y=ObsAdj, color=Type, shape=Month)) + geom_point(size=3) + geom_errorbar(limits)
+ labs(title="Observed Values vs Mout_1", x="Mout_1 (Kg/Day)", y="Observed Plastic Output (Kg/Day)") +
theme(plot.title=element_text(hjust=0.5)) ## + geom_abline(intercept = 0.0243, slope = -0.0268)

## Linear regression of Scaled Observed vs Scaled Mout1
require(stats)
regs1 <- lm(Scaled_Observed ~ Scaled_Mout1, data=TStats2)
regs1
summary(regs1)
shapiro.test(residuals(regs1))
ggplot(TStats2, aes(x=Scaled_Mout1, y=Scaled_Observed, color=Type, shape=Month)) + geom_point(size=3)+
labs(title="Scaled Observed Values vs Scaled Mout_1", x="Scaled Mout_1 (Kg/Day)", y="Scaled Observed Plastic
Output (Kg/Day)") + theme(plot.title=element_text(hjust=0.5)) ##  + geom_abline(intercept = -4.738e-17, slope = -
1.894e-01)

## Linear regression of Observed vs Mout2
require(stats)
reg2 <- lm(ObsAdj ~ Mout2, data=TStats2)
reg2
summary(reg2)
ggplot(TStats2, aes(x=Mout2, y=ObsAdj, color=Type, shape=Month)) + geom_point(size=3) + geom_errorbar(limits)
+labs(title="Observed Values vs Mout_2", x="Mout_2 (Kg/Day)", y="Observed Plastic Output (Kg/Day)") +
theme(plot.title=element_text(hjust=0.5)) ## + geom_abline(intercept = 0.0243, slope = -0.0135)

## Linear regression of Scaled Observed vs Scaled Mout2
require(stats)
regs3 <- lm(Scaled_Observed ~ Scaled_Mout2)
regs3
summary(regs3)
shapiro.test(residuals(regs3))
```

```r
ggplot(TStats2, aes(x=Scaled_Mout2, y=Scaled_Observed, color=Type, shape=Month)) + geom_point(size=3) + labs(title="Scaled Observed Values vs Scaled Mout_2", x="Scaled Mout_2 (Kg/Day)", y="Scaled Observed Plastic Output (Kg/Day)") + theme(plot.title=element_text(hjust=0.5)) ## + geom_abline(intercept = -5.234e-17, slope = -1.905e-01)

## Linear Regression between observed and EROM runoff
reg4 <- lm(ObsAdj ~ Runoff, data=TStats2)
reg4
summary(reg4)
ggplot(TStats2, aes(x=Runoff, y=ObsAdj, color=Type, shape=Month)) + geom_point(size=3) + geom_errorbar(limits, width=0.25) +labs(title="Observed Values vs Runoff", x="Runoff (MM/Day)", y="Observed Plastic Output (Kg/Day)") + theme(plot.title=element_text(hjust=0.5)) ## + geom_abline(intercept = 0.024372, slope = -0.0001666)

## Linear regression of Scaled Observed vs Scaled EROM Runoff
require(stats)
regs5 <- lm(Scaled_Observed ~ Scaled_Runoff)
regs5
summary(regs5)
shapiro.test(residuals(regs5))
ggplot(TStats2, aes(x=Scaled_Runoff, y=Scaled_Observed, color=Type, shape=Month)) + geom_point(size=3) + labs(title="Scaled Observed Values vs Scaled Runoff", x="Scaled Runoff (MM/Day)", y="Scaled Observed Plastic Output (Kg/Day)") + theme(plot.title=element_text(hjust=0.5)) ## + geom_abline(intercept = -4.684e-17, slope = -1.401e-01)

## Linear regression of Observed vs Population
reg6 <- lm(ObsAdj ~ Population, data=TStats2)
reg6
summary(reg6)
ggplot(TStats2, aes(x=Population, y=ObsAdj, color=Type, shape=Month)) + geom_point(size=3) + geom_errorbar(limits, width=0.25) + labs(title="Observed Values vs Population", x="Population", y="Observed Plastic Output (Kg/Day)") + theme(plot.title=element_text(hjust=0.5)) ## + geom_abline(intercept = 2.471e-02, slope = -2.803e-06)

## Linear regression of Scaled Observed vs Scaled Population
require(stats)
regs7 <- lm(Scaled_Observed ~ Scaled_Pop)
regs7
summary(regs7)
shapiro.test(residuals(regs7))
ggplot(TStats2, aes(x=Scaled_Pop, y=Scaled_Observed, color=Type, shape=Month)) + geom_point(size=3) + labs(title="Scaled Observed Values vs Scaled Population", x="Scaled Population", y="Scaled Observed Plastic Output (Kg/Day)") + theme(plot.title=element_text(hjust=0.5)) ## + geom_abline(intercept = -5.716e-17, slope = -1.842e-01)

## Two Way Anova (Factor 1 = month, Factor 2 = type [High,Medium,Low], Response is observed)
obs.ano <- aov (ObsAdj ~ as.factor(Month)*as.factor(Type), data=TStats2)
summary(obs.ano)
TukeyHSD(obs.ano)
sdob2 <- 0.0006752
limits2 <- aes(ymax = ObsAdj + sdob2, ymin = ObsAdj - sdob2)
limits2
TStats2.ano <- TStats2
TStats2.ano$Month <- factor(TStats2.ano$Month, levels = c("October","November","December"))
TStats2.ano$Type <- factor (TStats2.ano$Type, levels = c("Low", "Medium", "High"))
TStats2.ano
ggplot(TStats2.ano, aes(x=Month, y=ObsAdj, fill=Type)) + geom_bar(stat="identity", position = position_dodge()) + geom_errorbar(limits2, width=0 ,position=position_dodge(width=0.9)) + labs(x="Month", y="Observed Plastic Output (Kg/Day)")
```

Appendix H. Tukey Results

```
> TukeyHSD(obs.ano)
  Tukey multiple comparisons of means
    95% family-wise confidence level

Fit: aov(formula = ObsAdj ~ as.factor(Month) * as.factor(Type), data = TStats2)

$`as.factor(Month)`
                        diff          lwr         upr
November-December -0.008545333 -0.0225071196 0.005416453
October-December   0.004939200 -0.0090225862 0.018900986
October-November   0.013484533 -0.0004772529 0.027446320
                      p adj
November-December 0.2541175
October-December  0.6022944
October-November  0.0580200

$`as.factor(Type)`
                  diff         lwr        upr     p adj
Low-High    -0.0024308000 -0.01639259 0.01153099 0.8795457
Medium-High -0.0018809333 -0.01584272 0.01208085 0.9256060
Medium-Low   0.0005498667 -0.01341192 0.01451165 0.9933611

$`as.factor(Month):as.factor(Type)`
                                  diff         lwr        upr
November:High-December:High     -0.0072912 -0.04155599 0.02697359
October:High-December:High       0.0145824 -0.01968239 0.04884719
December:Low-December:High      -0.0049392 -0.03920399 0.02932559
November:Low-December:High      -0.0039996 -0.03826439 0.03026519
October:Low-December:High        0.0089376 -0.02532719 0.04320239
December:Medium-December:High    0.0115248 -0.02273999 0.04578959
November:Medium-December:High   -0.0077596 -0.04202439 0.02650519
October:Medium-December:High    -0.0021168 -0.03638159 0.03214799
October:High-November:High       0.0218736 -0.01239119 0.05613839
December:Low-November:High       0.0023520 -0.03191279 0.03661679
November:Low-November:High       0.0032916 -0.03097319 0.03755639
October:Low-November:High        0.0162288 -0.01803599 0.05049359
December:Medium-November:High    0.0188160 -0.01544879 0.05308079
November:Medium-November:High   -0.0004684 -0.03473319 0.03379639
October:Medium-November:High     0.0051744 -0.02909039 0.03943919
December:Low-October:High       -0.0195216 -0.05378639 0.01474319
November:Low-October:High       -0.0185820 -0.05284679 0.01568279
October:Low-October:High        -0.0056448 -0.03990959 0.02861999
December:Medium-October:High    -0.0030576 -0.03732239 0.03120719
November:Medium-October:High    -0.0223420 -0.05660679 0.01192279
October:Medium-October:High     -0.0166992 -0.05096399 0.01756559
November:Low-December:Low        0.0009396 -0.03332519 0.03520439
October:Low-December:Low         0.0138768 -0.02038799 0.04814159
December:Medium-December:Low     0.0164640 -0.01780079 0.05072879
November:Medium-December:Low    -0.0028204 -0.03708519 0.03144439
October:Medium-December:Low      0.0028224 -0.03144239 0.03708719
October:Low-November:Low         0.0129372 -0.02132759 0.04720199
December:Medium-November:Low     0.0155244 -0.01874039 0.04978919
November:Medium-November:Low    -0.0037600 -0.03802479 0.03050479
October:Medium-November:Low      0.0018828 -0.03238199 0.03614759
December:Medium-October:Low      0.0025872 -0.03167759 0.03685199
November:Medium-October:Low     -0.0166972 -0.05096199 0.01756759
October:Medium-October:Low      -0.0110544 -0.04531919 0.02321039
November:Medium-December:Medium -0.0192844 -0.05354919 0.01498039
```

```
October:Medium-December:Medium  -0.0136416 -0.04790639 0.02062319
October:Medium-November:Medium   0.0056428 -0.02862199 0.03990759
                                    p adj
November:High-December:High     0.9914619
October:High-December:High      0.7438692
December:Low-December:High      0.9993706
November:Low-December:High      0.9998636
October:Low-December:High       0.9716720
December:Medium-December:High   0.8982679
November:Medium-December:High   0.9875006
October:Medium-December:High    0.9999989
October:High-November:High      0.3288084
December:Low-November:High      0.9999976
November:Low-November:High      0.9999683
October:Low-November:High       0.6436779
December:Medium-November:High   0.4869061
November:Medium-November:High   1.0000000
October:Medium-November:High    0.9991262
December:Low-October:High       0.4470560
November:Low-October:High       0.5004921
October:Low-October:High        0.9984029
December:Medium-October:High    0.9999819
November:Medium-October:High    0.3082141
October:Medium-October:High     0.6145247
November:Low-December:Low       1.0000000
October:Low-December:Low        0.7844029
December:Medium-December:Low    0.6290986
November:Medium-December:Low    0.9999902
October:Medium-December:Low     0.9999902
October:Low-November:Low        0.8344483
December:Medium-November:Low    0.6871418
November:Medium-November:Low    0.9999138
October:Medium-November:Low     0.9999996
December:Medium-October:Low     0.9999950
November:Medium-October:Low     0.6146485
October:Medium-October:Low      0.9159298
November:Medium-December:Medium 0.4602543
October:Medium-December:Medium  0.7974016
October:Medium-November:Medium  0.9984068
```

References

Akovali, G. (2012). *Plastic materials: polyvinyl chloride (PVC). Toxicity of Building Materials, 23–53*. doi:10.1533/9780857096357.23

Aikoh, T. (2006). Monitoring Trampling Impacts in the Disposal of Human Waste at Campsites and Visitors' Attitudes to a Carry-out System. *Exploring the Nature of Management*, 436.

Bakir, A., Rowland, S. J., & Thompson, R. C. (2014). Transport of persistent organic pollutants by microplastics in estuarine conditions. *Estuarine, Coastal and Shelf Science*, *140*, 14-21.

Barrows, A. P. W., Neumann, C. A., Berger, M. L., & Shaw, S. D. (2017). Grab vs. neuston tow net: a microplastic sampling performance comparison and possible advances in the field. *Analytical Methods*, 9(9), 1446–1453. doi:10.1039/c6ay02387h.

Besseling, E., Quik, J. T., Sun, M., & Koelmans, A. A. (2017). Fate of nano-and microplastic in freshwater systems: A modeling study. *Environmental Pollution*, *220*, 540-548.

Bondelind, M., Nguyen, A., Sokolova, E., & Björklund, K. (2018, September). Transport of traffic-related microplastic particles in receiving water. In *International Conference on Urban Drainage Modelling* (pp. 317-321). Springer, Cham.

Centers for Disease Control and Prevention/ Agency for Toxic Substances and Disease Registry/ Geospatial Research, Analysis, and Services Program (GRASP). CDC Social Vulnerability Index 2018 Database Louisiana. https://www.atsdr.cdc.gov/placeandhealth/svi/data_documentation_download.html. Accessed on August 1 2020.

Cowles, A., Willson, C., & Twilley, R. (2019). Effects of Land-Use Change (1938–2018) on Surface Runoff and Flooding in the Amite River Basin, Louisiana, USA Using Coupled 1D/2D HEC-RAS–HEC-HMS Hydrological Modeling. *Earth and Space Science Open Archive*. Retrieved March 13, 2021.

Crawford, C. B., & Quinn, B. (Eds.), *Microplastic Pollutants*. Elsevier Limited. pp. 57-100.

Dermansky, J. (2020, August 28). Pollution scientist Calls PLASTIC Pellet spill in the Mississippi River 'a Nurdle apocalypse'. Retrieved February 18, 2021, fromhttps://www.desmogblog.com/2020/08/28/new-orleans-louisiana-plastic-spill-mississippi-river-nurdle-apocalypse.

Deshpande, P. C., Philis, G., Brattebø, H., & Fet, A. M. (2020). Using Material Flow Analysis (MFA) to generate the evidence on plastic waste management from commercial fishing gears in Norway. *Resources, Conservation & Recycling: X*, *5*, 100024.

Dutzik, T., Crowell, P., & Rumpler, J. (2009). Wasting Our Waterways. *Environment America Research & Policy Center*. Fall 2009.

Flowers M (2016). Zooming in on the five types of microplastics. http://www.waterkeeper.ca/blog/2016/11/15/zooming-in-on-the-five-types-of-microplastic. Accessed 12 December 2020.

Freeman, S., Booth, A. M., Sabbah, I., Tiller, R., Dierking, J., Klun, K., ... & Angel, D. L. (2020). Between source and sea: The role of wastewater treatment in reducing marine microplastics. *Journal of Environmental Management*, *266*, 110642.

Gaffin, S. R., Rosenzweig, C., Xing, X., & Yetman, G. (2004). Downscaling and geo-spatial gridding of socio-economic projections from the IPCC Special Report on Emissions Scenarios (SRES). *Global Environmental Change*, *14*(2), 105-123.

Galgani, F., Leaute, J. P., Moguedet, P., Souplet, A., Verin, Y., Carpentier, A., ... & Nerisson, P. (2000). Litter on the sea floor along European coasts. *Marine Pollution Bulletin*, *40*(6), 516-527.

Galloway, T. S., Cole, M., & Lewis, C. (2017). Interactions of microplastic debris throughout the marine ecosystem. *Nature Ecology & Evolution*, *1*(5), 1-8.

General Oceanics, 2018, 2030 and 2031 Series Mechanical and Electronic Digital Flowmeter Operators Manual, 1st edition. General Oceanics, Inc. Miami, Fl, USA, May 2018. 5-7. Accessed on: February, 24, 2021. [Online]. https://www.generaloceanics.com/uploads/Files/2030%20MANUAL.pdf**.**

Harrison, J. P., Hoellein, T. J., Sapp, M., Tagg, A. S., Ju-Nam, Y., & Ojeda, J. J. (2018). Microplastic-associated biofilms: a comparison of freshwater and marine environments. In *Freshwater Microplastics* (pp. 181-201). Springer, Cham.

Horton, A. A., Svendsen, C., Williams, R. J., Spurgeon, D. J., & Lahive, E. (2017). Large microplastic particles in sediments of tributaries of the River Thames, UK–Abundance, sources and methods for effective quantification. *Marine Pollution Bulletin*, *114*(1), 218-226.

Hurley, R., Woodward, J., & Rothwell, J. J. (2018). Microplastic contamination of river beds significantly reduced by catchment-wide flooding. Nature Geoscience, 11(4), 251-257.

Jambeck, J. R., Geyer, R., Wilcox, C., Siegler, T. R., Perryman, M., Andrady, A., Narayan, R., & Law, K. L. (2015). Plastic waste inputs from land into the ocean. *Science*, 347(6223), 768-771.

Karian, H. (Ed.). (2003). *Handbook of polypropylene and polypropylene composites, revised and expanded*. CRC press.

Kataoka, T., Nihei, Y., Kudou, K., & Hinata, H. (2019). Assessment of the sources and inflow processes of microplastics in the river environments of Japan. *Environmental Pollution*, *244*, 958-965.

Kole, P. J., Löhr, A. J., Van Belleghem, F. G., & Ragas, A. M. (2017). Wear and tear of tyres: a stealthy source of microplastics in the environment. *International Journal of Environmental Research and Public Health*, *14*(10), 1265.

Kowalski, N., Reichardt, A. M., & Waniek, J. J. (2016). Sinking rates of microplastics and potential implications of their alteration by physical, biological, and chemical factors. *Marine Pollution Bulletin*, *109*(1), 310-319.

Lebreton, L. C., Van Der Zwet, J., Damsteeg, J. W., Slat, B., Andrady, A., & Reisser, J. (2017). River plastic emissions to the world's oceans. *Nature Communications*, 8, 15611.

Leung, Y. F., & Marion, J. L. (2004). Managing impacts of camping. *Environmental Impacts of Ecotourism. Wallingford: CABI.*

Li, J., Liu, H., & Chen, J. P. (2018). Microplastics in freshwater systems: A review on occurrence, environmental effects, and methods for microplastics detection. *Water Research*, 137, 362-374.

LI, W. C., Tse, H. F., & Fok, L. (2016). Plastic waste in the marine environment: A review of sources, occurrence and effects. *Science of the Total Environment*, *566*, 333-349.

Liu, G., Zhu, Z., Yang, Y., Sun, Y., Yu, F., & Ma, J. (2019). Sorption behavior and mechanism of hydrophilic organic chemicals to virgin and aged microplastics in freshwater and seawater. *Environmental Pollution*, *246*, 26-33.

Martin, K. M. (2018, August 1). Quantifying and characterizing the Mississippi River's contribution of microplastic debris to the Gulf of Mexico. Ph.D Dissertaion, Texas A&M University, College Station Texas. 5-6. https://tamucc-ir.tdl.org/handle/1969.6/87095.

Mato, Y., Isobe, T., Takada, H., Kanehiro, H., Ohtake, C., & Kaminuma, T. (2001). Plastic resin pellets as a transport medium for toxic chemicals in the marine environment. *Environmental Science & Technology*, *35*(2), 318-324.

McKay, L., Bondelid, T., Dewald, T., Johnston, J., Moore, R., and Rea, A., "NHDPlus Version 2: User Guide", 2012.

Müller, Y. K., Wernicke, T., Pittroff, M., Witzig, C. S., Storck, F. R., Klinger, J., & Zumbülte, N. (2020). Microplastic analysis—are we measuring the same? Results on the first global comparative study for microplastic analysis in a water sample. *Analytical and Bioanalytical Chemistry*, *412*(3), 555-560.

Munno, K., Helm, P. A., Jackson, D. A., Rochman, C., & Sims, A. (2018). Impacts of temperature and selected chemical digestion methods on microplastic particles. *Environmental Toxicology and Chemistry*, *37*(1), 91-98.

National inventory of dams. Washington, DC :US Army Corps of Engineers : Federal Emergency Management Agency. https://nid.sec.usace.army.mil/ords/f?p=105:113:7869877641222::NO:113,2:P113_STATE,P113_COUNTY:LA,033.

Naqash, N., Prakash, S., Kapoor, D., & Singh, R. (2020). Interaction of freshwater microplastics with biota and heavy metals: a review. *Environmental Chemistry Letters*, 1-12.

Parker, D. (2013, July 18). Plastics: OR&R's Marine Debris Program. Retrieved April 11, 2020, from https://marinedebris.noaa.gov/info/plastic.html.

Prata, J. C., da Costa, J. P., Duarte, A. C., & Rocha-Santos, T. (2019). Methods for sampling and detection of microplastics in water and sediment: A critical review. *TrAC Trends in Analytical Chemistry*, *110*, 150-159.

Program, N. O. S. O. R. R. M. D. (2020, April 10). Types and Sources. Retrieved April 11, 2020, from https://marinedebris.noaa.gov/discover-issue/types-andsources.

Rios, L. M., Moore, C., & Jones, P. R. (2007). Persistent organic pollutants carried by synthetic polymers in the ocean environment. *Marine Pollution Bulletin*, *54*(8), 1230-1237.

R Core Team. 2020. R: A language and environment for statistical computing. R Foundation for Statistical Computing, Vienna, Austria. URL https://www.R-project.org/.

Scircle, A., Cizdziel, J. V., Missling, K., Li, L., & Vianello, A. (2020). Single-Pot Method for the Collection and Preparation of Natural Water for Microplastic Analyses: Microplastics in the Mississippi River System during and after Historic Flooding. *Environmental Toxicology and Chemistry*, *39*(5), 986-995.

Shim, W. J., Hong, S. H., & Eo, S. E. (2017). Identification methods in microplastic analysis: a review. *Analytical Methods*, *9*(9), 1384-1391.

Sleeter, R., & Gould, M. D. (2007). *Geographic information system software to remodel population data using dasymetric mapping methods*. US Department of the Interior, US Geological Survey.

Srivastava, R. K., & Godara, S. (2017). Use of polycarbonate plastic products and human health. *Int J Basic Clin Pharmacol*, *2*(1), 12-17.

Sun, X., Li, Q., Zhu, M., Liang, J., Zheng, S., & Zhao, Y. (2017). Ingestion of microplastics by natural zooplankton groups in the northern South China Sea. *Marine Pollution Bulletin*, *115*(1-2), 217-224.

Tibbetts, J., Krause, S., Lynch, I., & Sambrook Smith, G. H. (2018). Abundance, distribution, and drivers of microplastic contamination in urban river environments. *Water*, *10*(11), 1597.

Toner, K. E., "Identification and Quantification of Microplastic Pollution in Water Samples and Four Species of Fish from the Mississippi River" (2020). *LSU Master's Theses*. 5184. https://digitalcommons.lsu.edu/gradschool_theses/5184.

USGS. U.S. Geological Survey. National Hydrography Dataset high-resolution flowline data. https://viewer.nationalmap.gov/advanced-viewer/. Last updated 22 October 2018. Accessed 18 December 2020.

Van Melkebeke, M., Janssen, C., & De Meester, S. (2020). Characteristics and sinking behavior of typical microplastics including the potential effect of biofouling: implications for remediation. *Environmental Science & Technology*, *54*(14), 8668-8680.

Wang, S. Y., Mao, Q. J., Xia, Z. D., ZHONG, T. X., & DING, T. (2007). Recycling of Polycarbonate Plastic. *Journal of Synthetic Crystals*, *36*(1), 195.

Wehle, D. H. S., & Coleman, F. C. (1983). Plastics at sea. Natural History, 2(83), 20-26.

Willson, C. (2017). Watershed at Amite River, Denham Springs, LA, USA, HydroShare, http://www.hydroshare.org/resource/306bb9e067674103a89678858aa54b29.

Worm, B., Lotze, H. K., Jubinville, I., Wilcox, C., & Jambeck, J. (2017). Plastic as a persistent marine pollutant. *Annual Review of Environment and Resources*, 42, 1-26.

Wright, S. L., Thompson, R. C., & Galloway, T. S. (2013). The physical impacts of microplastics on marine organisms: a review. *Environmental pollution*, *178*, 483-492.

Yetman, G., Gaffin, S. R., & Xing, X. (2004). Global 15 x 15 Minute Grids of the Downscaled GDP Based on the SRES B2 Scenario, 1990 and 2025. Palisades, NY: NASA Socioeconomic Data and Applications Center (SEDAC).

Zhang, K., Hamidian, A. H., Tubić, A., Zhang, Y., Fang, J. K., Wu, C., & Lam, P. K. (2021). Understanding plastic degradation and microplastic formation in the environment: A review. *Environmental Pollution*, 116554.

80 FR 37053.

85 FR 22250.

33 U.S.C. §1251-1387.

Vita

Gourav Divan was born in Madison, Wisconsin, but was raised in Wisconsin, Atlanta, Georgia and San Jose, California. He graduated from Oakwood High School in 2014. After high school, he attended Louisiana State University, graduating in 2019 and earning the degrees of a Bachelors of Science in Coastal and Environmental Sciences, focusing on Applied Environmental Sciences, with a minor in Environmental Management Systems. He plans to receive his Masters August 2021, and after graduating from Louisiana State University, he will search for a job regarding water quality and assessment with aspects of citizen science. Outside of the laboratory, Gourav loves to play video games, work out, and cook.